

# XIII Ciclo de Cursos Especiais

27 a 31 de outubro de 2008

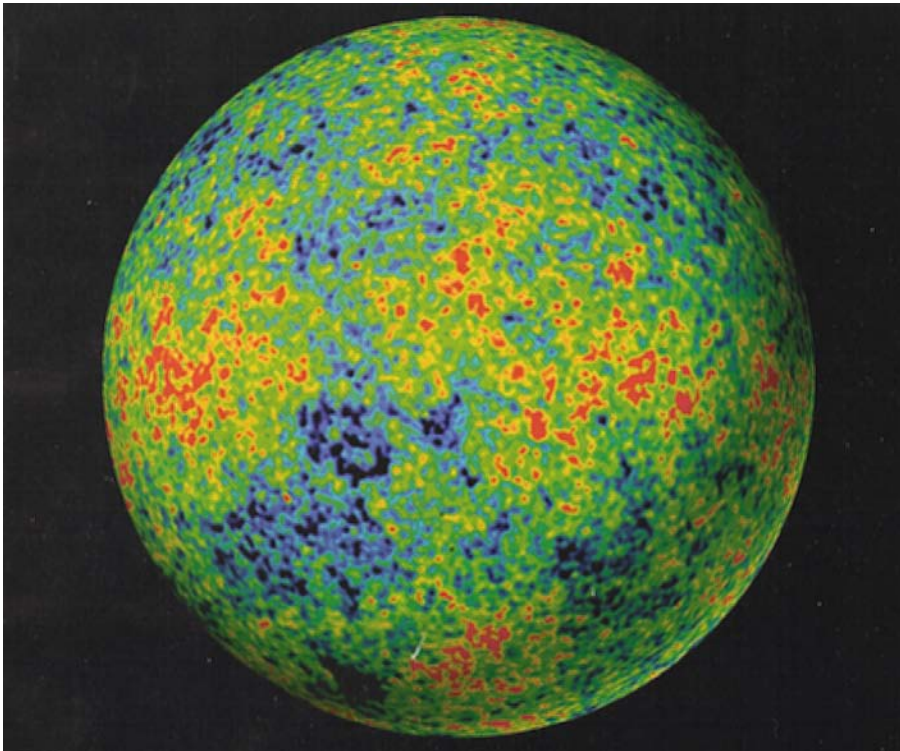
## Lecture 2 - Structure Formation in a $\Lambda$ CDM Universe

Joel Primack, UCSC

The  $\Lambda$ CDM “Double Dark” standard cosmological model is the basis of modern theories of the formation of galaxies, clusters, and larger scale structures in the universe. This lecture begins by showing that predictions of the  $\Lambda$ CDM model regarding the distribution of galaxies both nearby and out to high redshifts are in excellent agreement with observations. However, on sub-galactic scales there are several potential problems, summarized here under the rubrics satellites, cusps, and angular momentum. Although much work remains before any of these issues can be regarded as resolved, recent progress suggests that all of them may be less serious than once believed.

# GRAVITY – The Ultimate Capitalist Principle

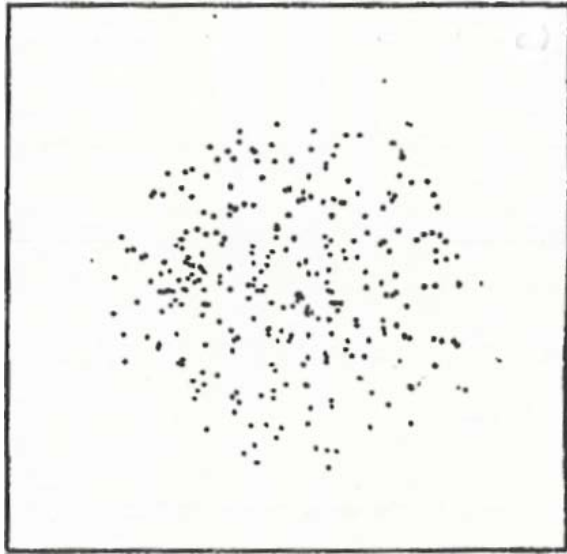
Astronomers say that a region of the universe with more matter is “richer.” Gravity magnifies differences—if one region is slightly denser than average, it will expand slightly more slowly and grow relatively denser than its surroundings, while regions with less than average density will become increasingly less dense. The rich always get richer, and the poor poorer.



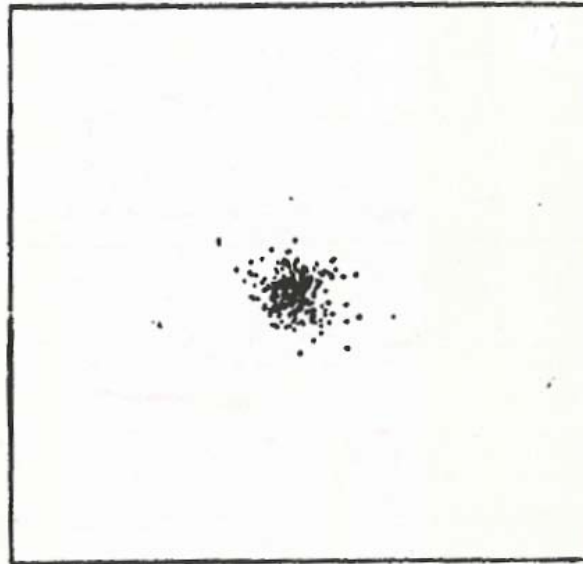
Temperature map at 380,000 years after the Big Bang. **Blue** (cooler) regions are slightly denser.  
From NASA's **WMAP** satellite, 2003.

The early universe expands *almost* perfectly uniformly. But there are small differences in density from place to place (about 30 parts per million). Because of gravity, denser regions expand more slowly, less dense regions more rapidly. Thus gravity amplifies the contrast between them, until...

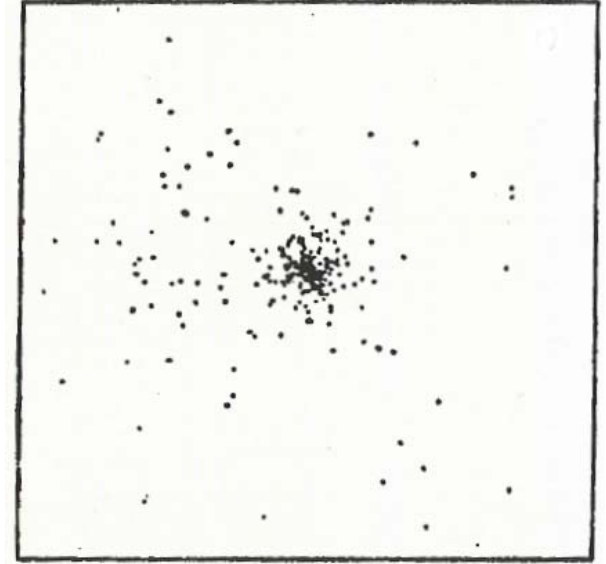
# Structure Formation by Gravitational Collapse



When any region becomes about twice as dense as typical regions its size, it reaches a maximum radius, *stops expanding*,



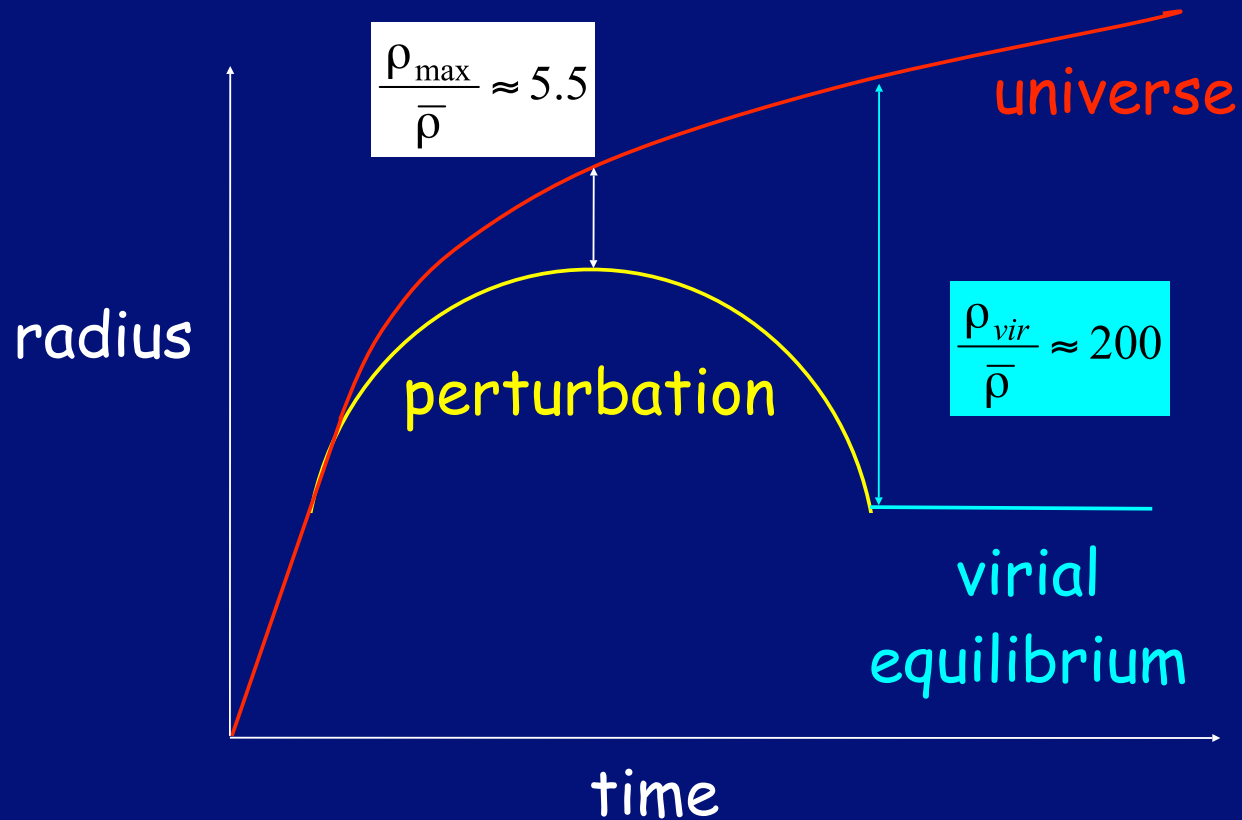
and starts falling together. The forces between the subregions generate velocities which *prevent* the material from *all falling toward the center*.



Through Violent Relaxation the dark matter quickly reaches a *stable configuration* that's about half the maximum radius but denser in the center.

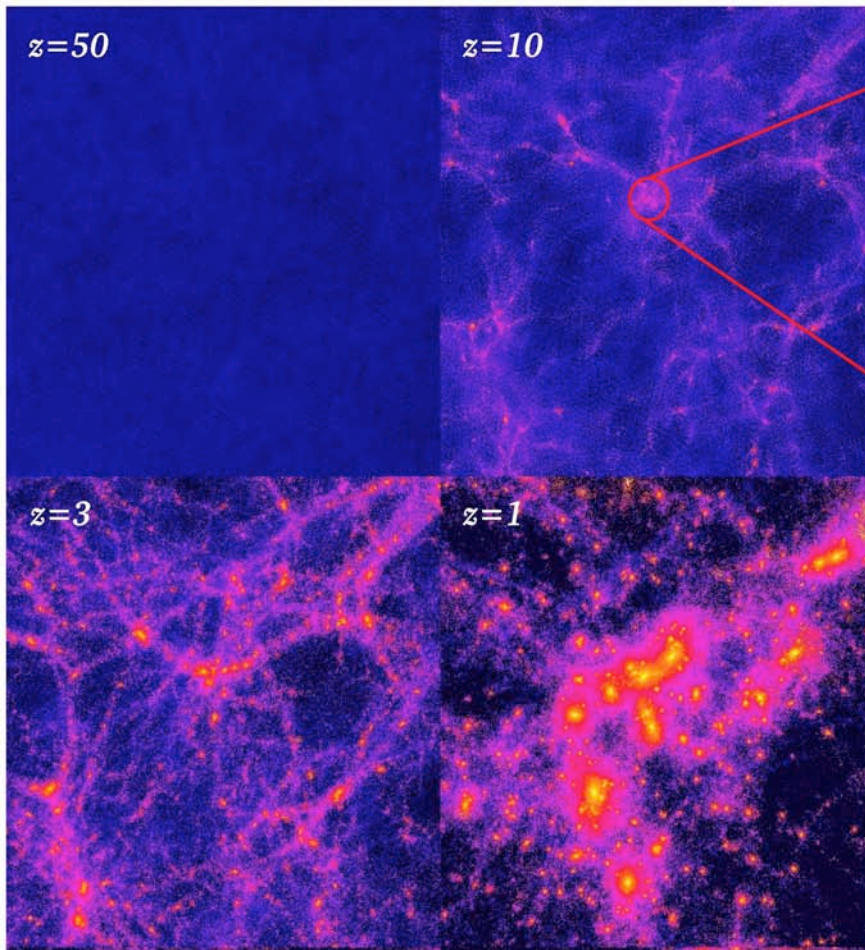
Simulation of top-hat collapse:  
P.J.E. Peebles 1970, ApJ, 75, 13.

# Spherical Collapse

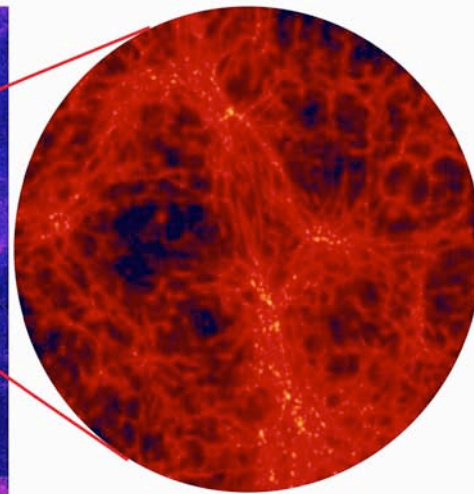
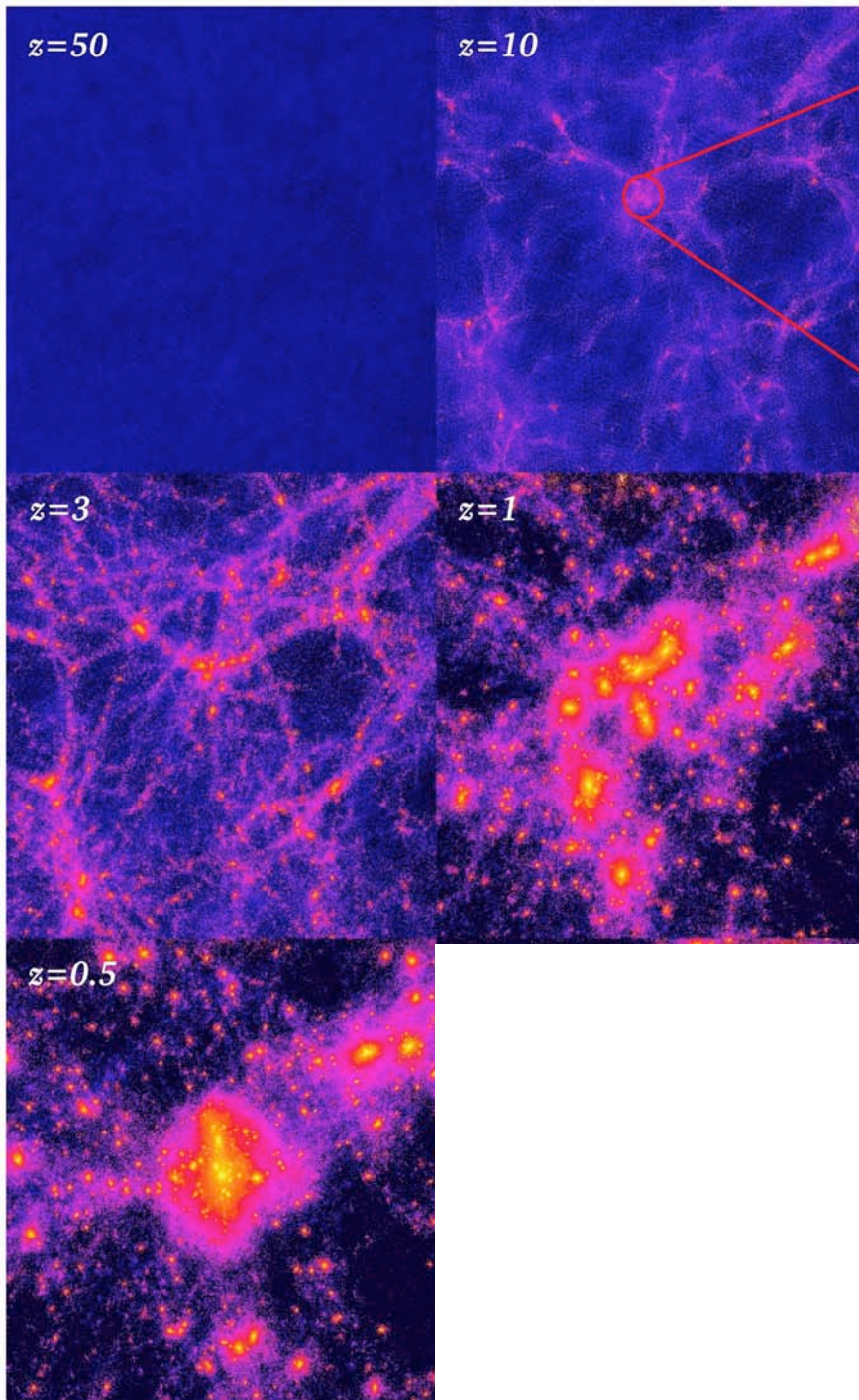


virial equilibrium:

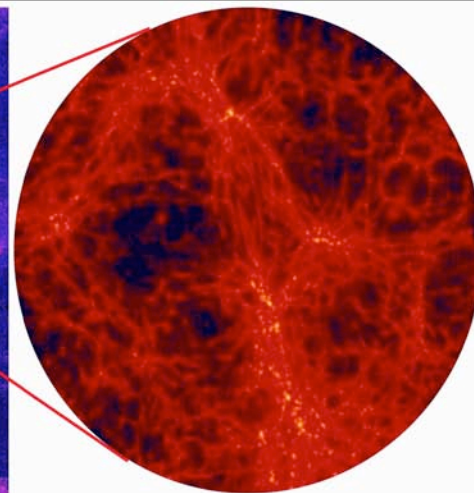
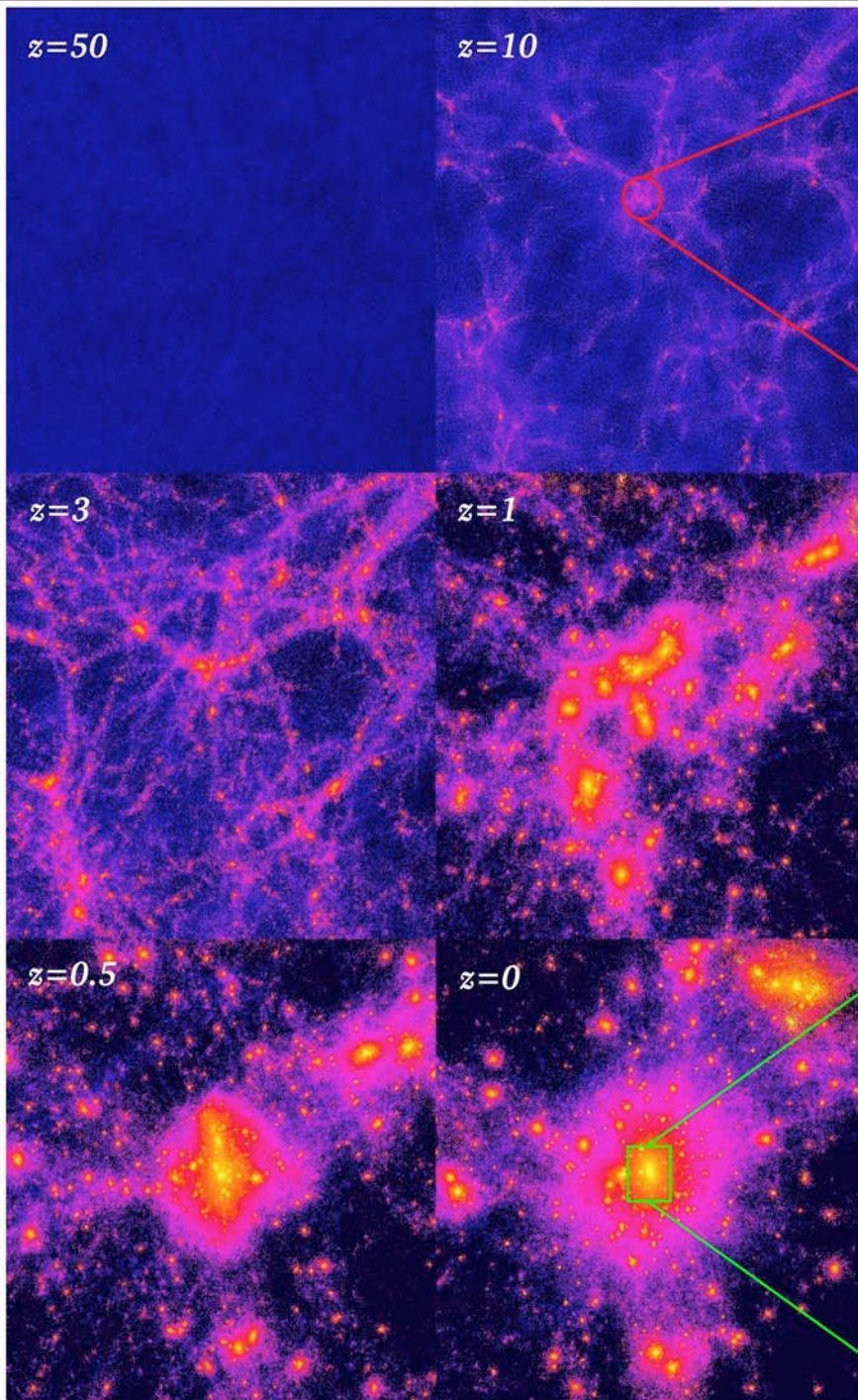
$$E = -\frac{1}{2} \frac{GM}{R_{vir}} = -\frac{GM}{R_{\max}}$$



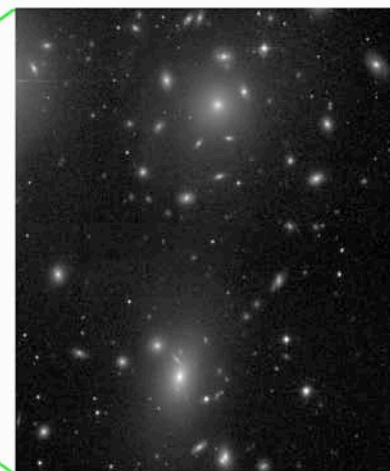
spherical collapse  
or mergers



spherical collapse  
or mergers

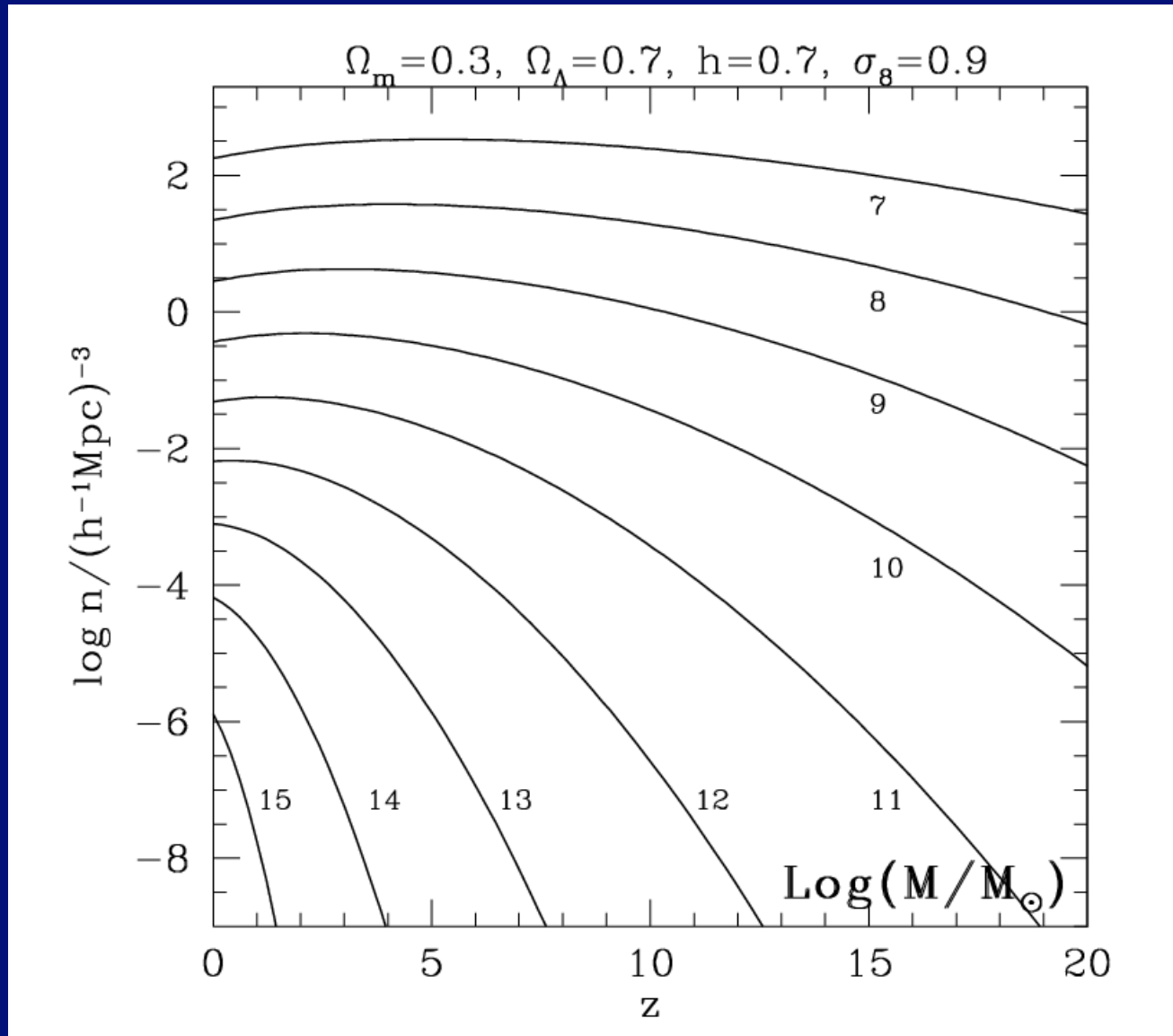


spherical collapse  
or mergers



# Halo Number Density vs. Redshift

## Sheth-Tormann Improved Press-Schechter



Mo &  
White  
2002



We define the characteristic properties of a dark halo within a sphere of radius  $r_{200}$  chosen so that the mean enclosed density is 200 times the mean cosmic value. Then

$$r_{200} = \left[ \frac{GM}{100\Omega_m(z)H^2(z)} \right]^{1/3}, \quad \text{and} \quad V_c = \left( \frac{GM}{r_{200}} \right)^{1/2}, \quad R(M) \equiv \left( \frac{3M}{4\pi\bar{\rho}_0} \right)^{1/3}, \quad \sigma^2(R) = \frac{1}{2\pi^2} \int_0^\infty k^3 P(k) \tilde{W}^2(kR) \frac{dk}{k}, \quad (1)$$

According to the argument first given by Press & Schechter (1974, hereafter PS), the abundance of haloes as a function of mass and redshift, expressed as the number of haloes per unit comoving volume at redshift  $z$  with mass in the interval  $(M, M + dM)$ , may be written as

$$n(M, z) dM = \sqrt{\frac{2\bar{\rho}_0}{\pi}} \frac{d\nu}{M dM} \exp\left(-\frac{\nu^2}{2}\right) dM. \quad (9)$$

Here  $\nu \equiv \delta_c/[D(z)\sigma(M)]$ , where  $\delta_c \approx 1.69$  and the growth factor is  $D(z) = g(z)/[g(0)(1+z)]$  with

$$g(z) \approx \frac{5}{2} \Omega_m \left[ \Omega_m^{4/7} - \Omega_\Lambda + (1 + \Omega_m/2)(1 + \Omega_\Lambda/70) \right]^{-1}, \quad \Omega_m \equiv \Omega_m(z), \quad \Omega_\Lambda \equiv \Omega_\Lambda(z) = \frac{\Omega_{\Lambda,0}}{E^2(z)}.$$

$$E(z) = \left[ \Omega_{\Lambda,0} + (1 - \Omega_0)(1+z)^2 + \Omega_{m,0}(1+z)^3 \right]^{1/2}. \quad \leftarrow \text{Lahav, Lilje, Primack, & Rees 1991}$$

Press & Schechter derived the above mass function from the *Ansatz* that the fraction  $F$  of all cosmic mass which at redshift  $z$  is in haloes with masses exceeding  $M$  is *twice* the fraction of randomly placed spheres of radius  $R(M)$  which have linear overdensity at that time exceeding  $\delta_c$ , the value at which a spherical perturbation collapses. Since the linear fluctuation distribution is gaussian this hypothesis implies

$$F(> M, z) = \text{erfc}\left(\frac{\nu}{\sqrt{2}}\right), \quad (12)$$

and equation (9) then follows by differentiation.

Numerical simulations show that although the scaling properties implied by the PS argument hold remarkably well for a wide variety of hierarchical cosmologies, substantially better fits to simulated mass functions are obtained if the error function in equation (12) is replaced by a function of slightly different shape. Sheth & Tormen (1999) suggested the following modification of equation (9)

$$n(M, z)dM = A \left(1 + \frac{1}{\nu'^{2q}}\right) \sqrt{\frac{2}{\pi}} \frac{\bar{\rho}}{M} \frac{d\nu'}{dM} \exp\left(-\frac{\nu'^2}{2}\right) dM, \quad (14)$$

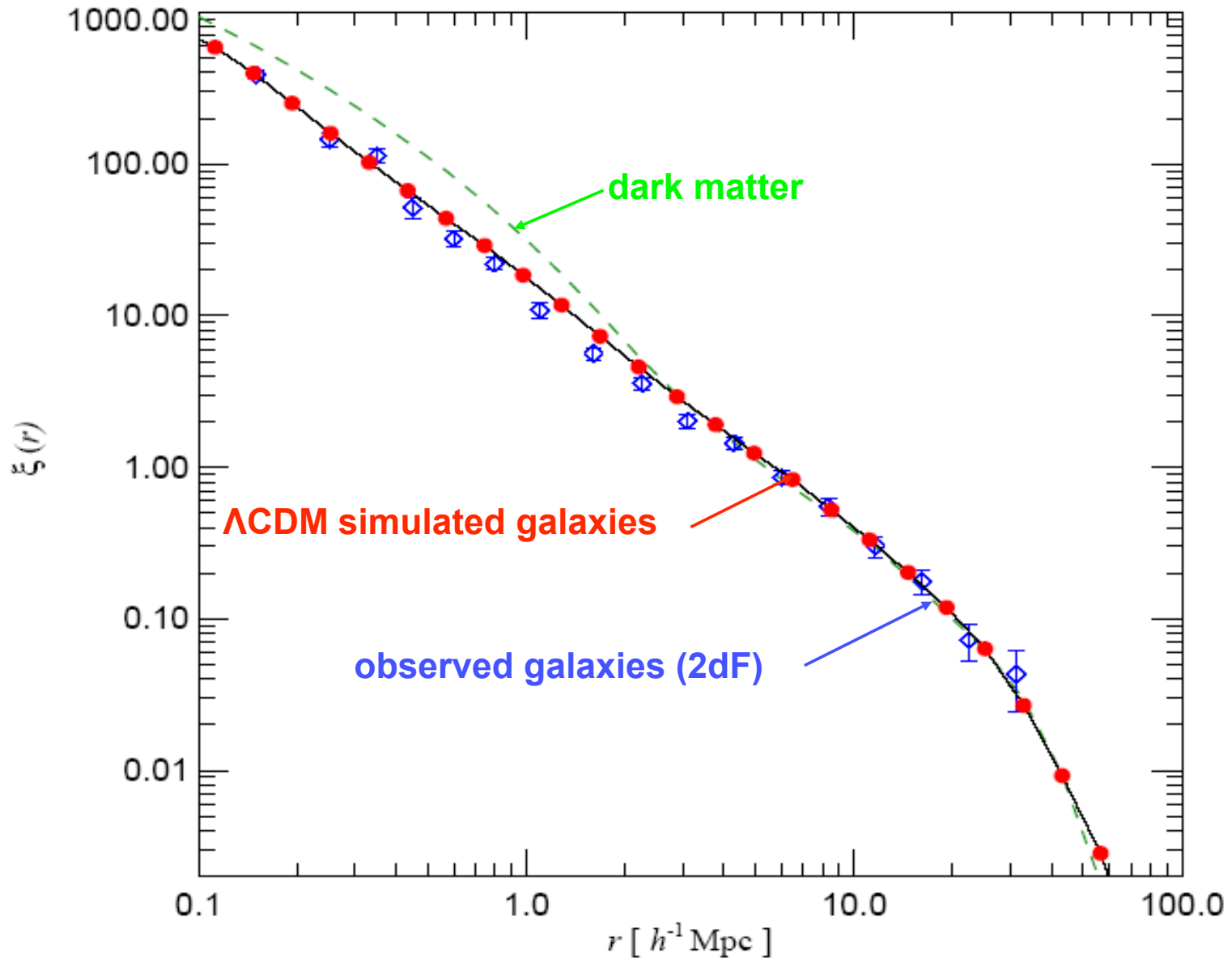
where  $\nu' = \sqrt{a}\nu$ ,  $a = 0.707$ ,  $A \approx 0.322$  and  $q = 0.3$ .

[See Sheth, Mo & Tormen (2001) and Sheth & Tormen (2002) for a justification of this formula in terms of an ellipsoidal model for perturbation collapse.] The fraction of all matter in haloes with mass exceeding  $M$  can be obtained by integrating equation (14). To good approximation,

$$F(> M, z) \approx 0.4 \left(1 + \frac{0.4}{\nu^{0.4}}\right) \operatorname{erfc}\left(\frac{0.85\nu}{\sqrt{2}}\right)$$

In a detailed comparison with a wide range of simulations, Jenkins et al. (2001) confirmed that this model is indeed a good fit provided haloes are defined at the same density contrast relative to the mean in all cosmologies. This is the reason behind our choice of definition for  $r_{200}$  in equation (1).

# UNDERSTANDING GALAXY CORRELATIONS



Galaxy 2-point correlation function at the present epoch.

Springel et al. 2005

**$\Lambda$ CDM  
PREDICTS  
EVOLUTION  
IN THE GALAXY  
CORRELATION  
FUNCTION**

$\xi_{gg}(r)$

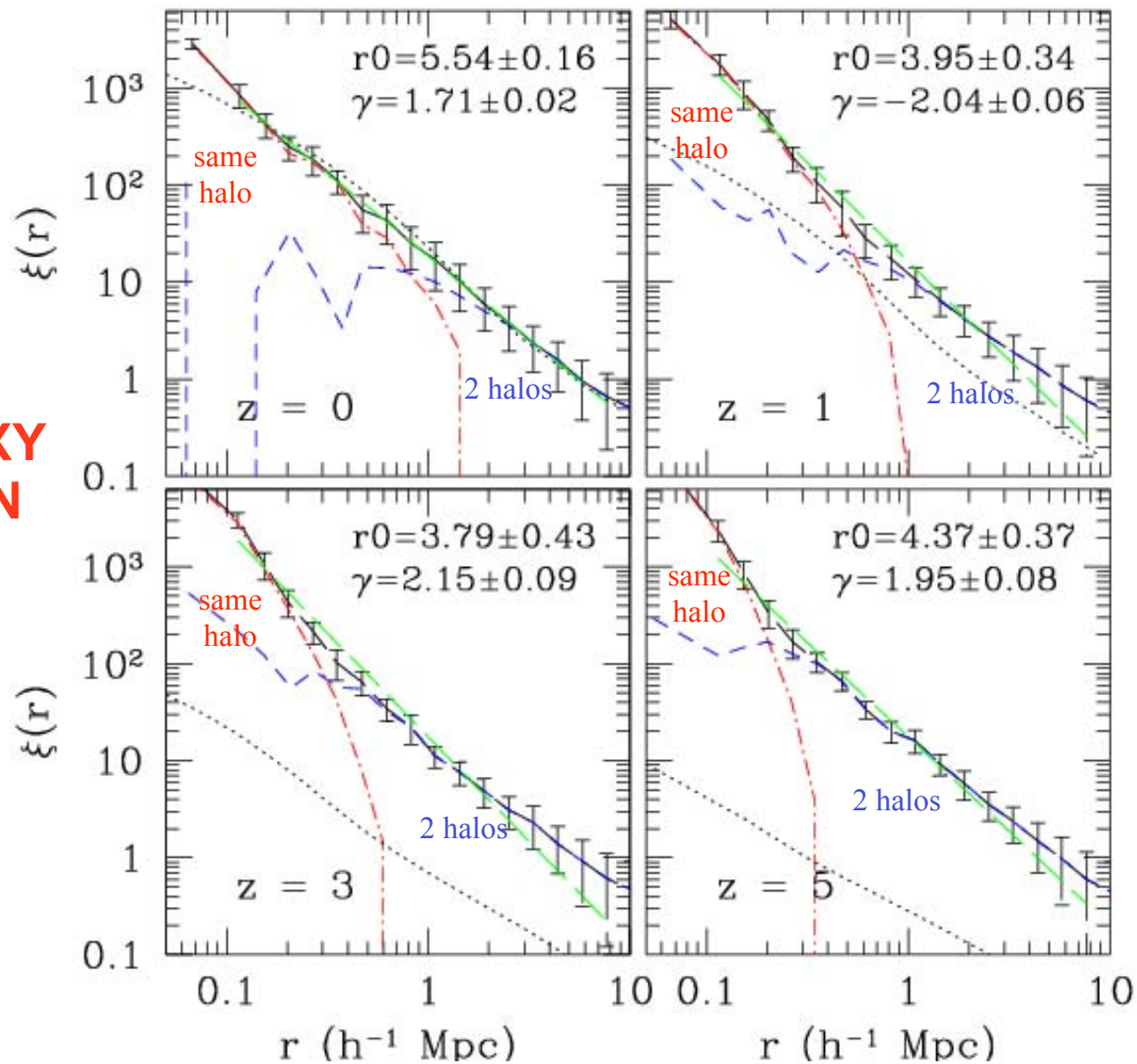
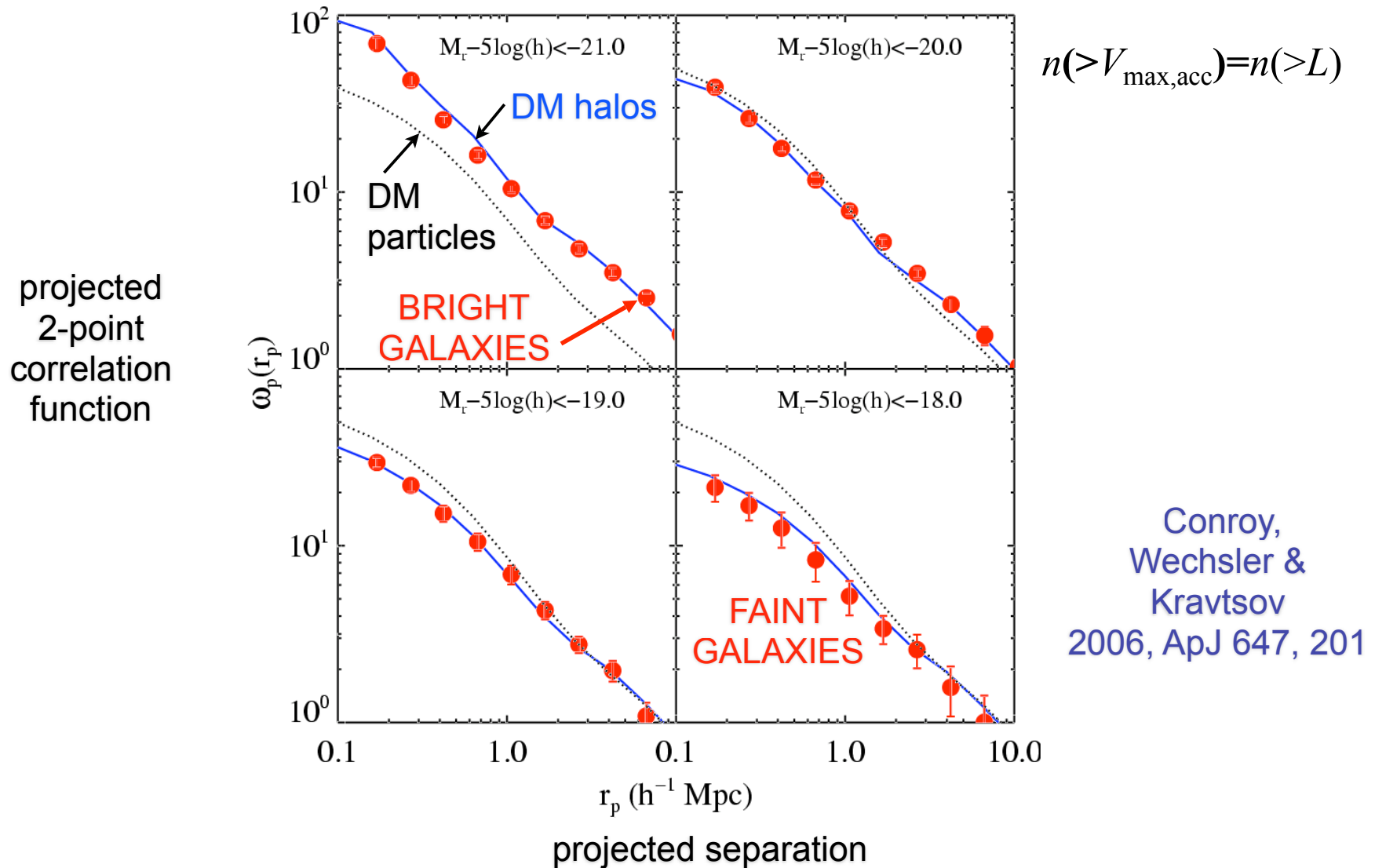


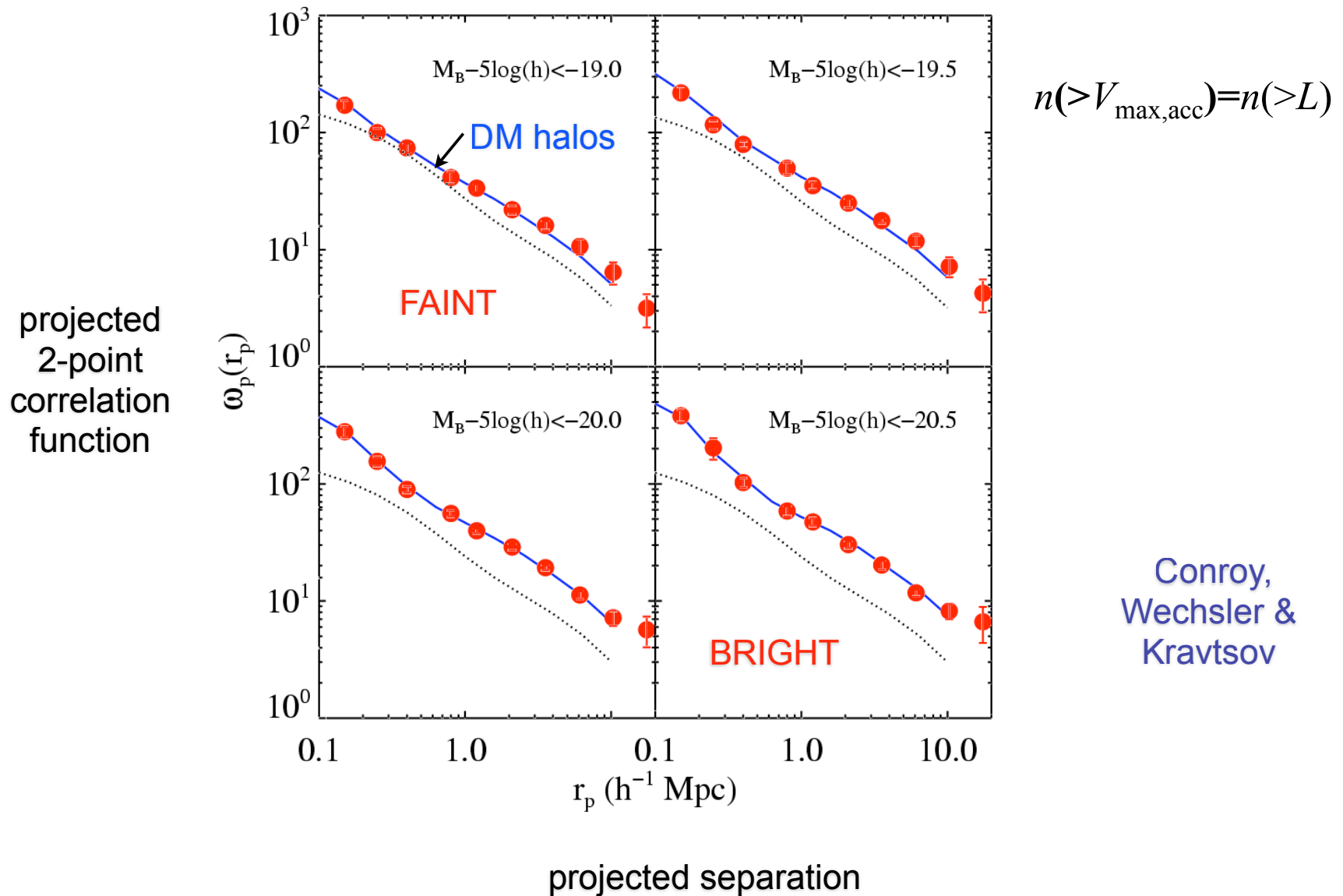
FIG. 8.— Evolution of the two-point correlation function in the  $80h^{-1}$  Mpc simulation. The solid line with error bars shows the clustering of halos of the fixed number density  $n = 5.89 \times 10^{-3} h^3 \text{ Mpc}^{-3}$  at each epoch. The error-bars indicate the “jack-knife” one sigma errors and are larger than the Poisson error at all scales. The dot-dashed and dashed lines show the corresponding one- and two-halo term contributions. The long-dashed lines show the power-law fit to the correlation functions in the range of  $r = [0.1 - 8h^{-1} \text{ Mpc}]$ . Although the correlation functions can be well fit by the power law at  $r \gtrsim 0.3h^{-1} \text{ Mpc}$  in each epoch, at  $z > 0$  the correlation function steepens significantly at smaller scales due to the one-halo term.

Kravtsov, Berlind, Wechsler, Klypin, Gottloeber, Allgood, & Primack 2004

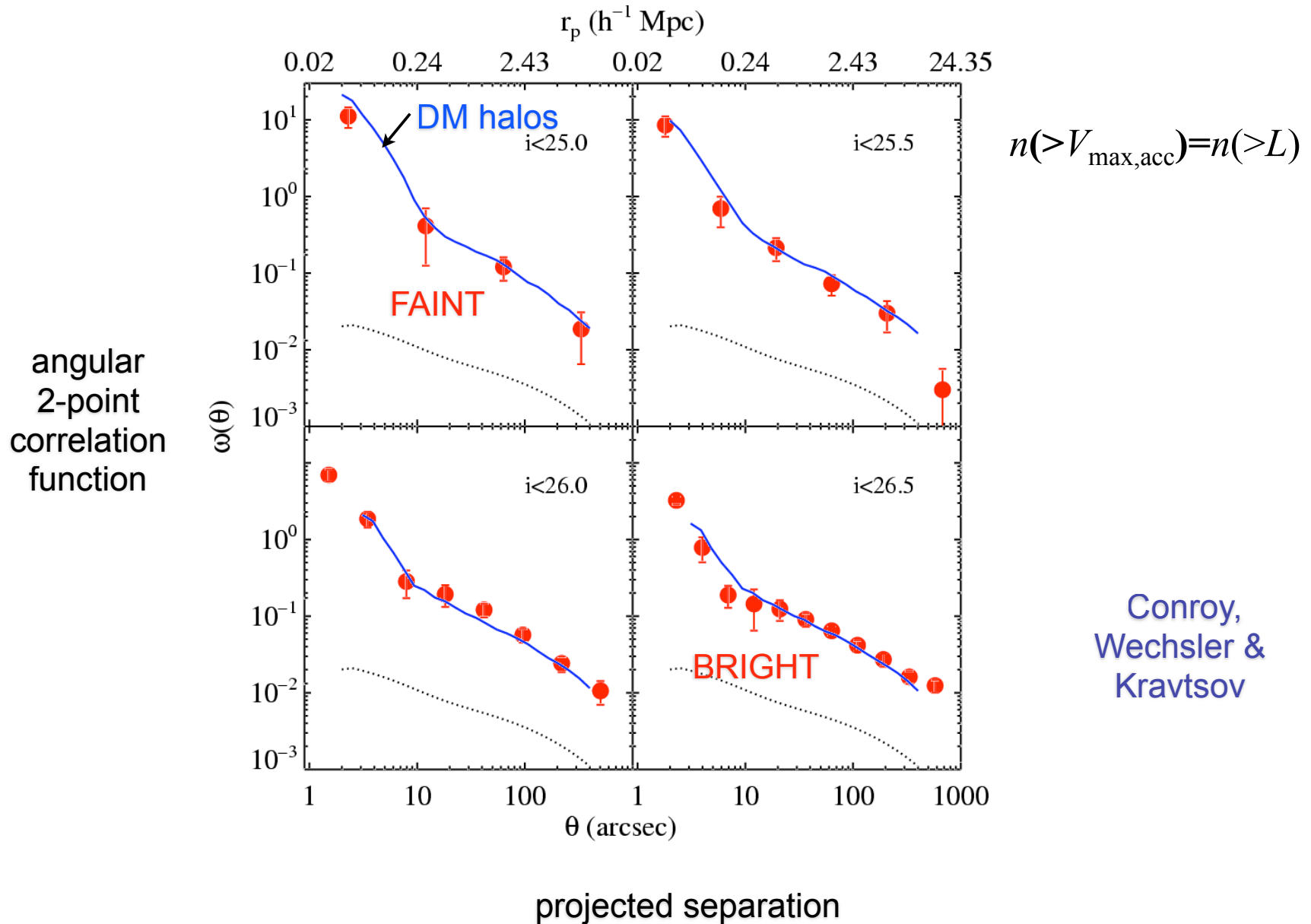
# Galaxy clustering in SDSS at $z \sim 0$ agrees with $\Lambda$ CDM simulations



# and at redshift $z \sim 1$ (DEEP2)!



# and at $z \sim 4-5$ (LBGs, Subaru)!!



# New Large Scale Data Keeps Agreeing with $\Lambda$ CDM Predictions

- Galaxy Clusters
  - Numbers, Baryon Fractions Allen+04
- SDSS Ly alpha forest  $P(k)$ 
  - McDonald+05, Seljak+06  $\sum m_\nu < 0.17 \text{ eV}$
- Baryon Acoustic Oscillations
  - 2dF Cole+05
  - SDSS Eisenstein+05
- Measurements of Cosmic Acceleration
  - Supernova Legacy Survey Astier+06
- Cosmic shear field
  - Canada-France-Hawaii Legacy Survey Hoekstra+06



small scale issues

Satellites

Cusps

Angular momentum

# Satellites: radial distribution

Simon White proposed that the observed bright satellite galaxies are hosted by the **most massive subhalos**, but this incorrectly predicts too large a radial distribution for the satellite galaxies in  $\Lambda$ CDM.

# Satellites: radial distribution

Simon White proposed that the observed bright satellite galaxies are hosted by the **most massive subhalos**, but this incorrectly predicts too large a radial distribution for the satellite galaxies in  $\Lambda$ CDM.

Andrey Kravtsov proposed instead that bright satellite galaxies are hosted by the **subhalos that were the most massive when they were accreted**.

This correctly predicts the observed radial distribution, and also explains why nearby satellites are dSph while more distant ones are a mix of dSph and dlrr galaxies.

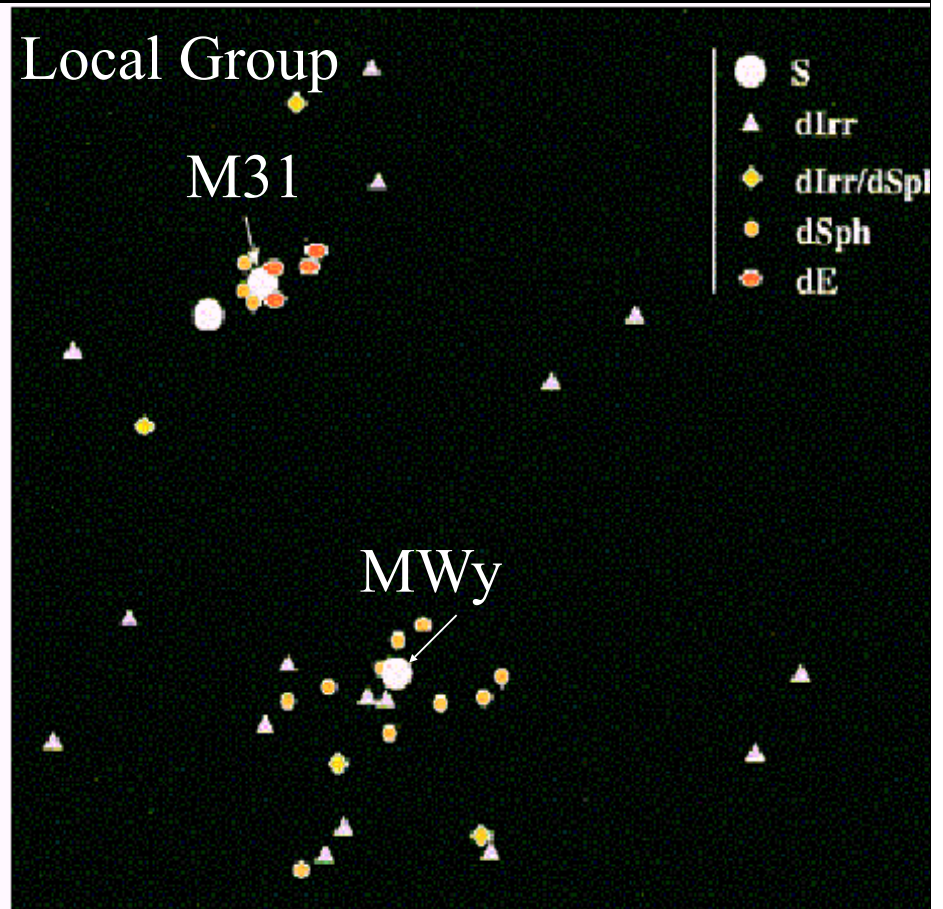
# Can the **large** number of small- $V_{\text{circ}}$ subhalos be reconciled with the **small** number of faint galaxies?

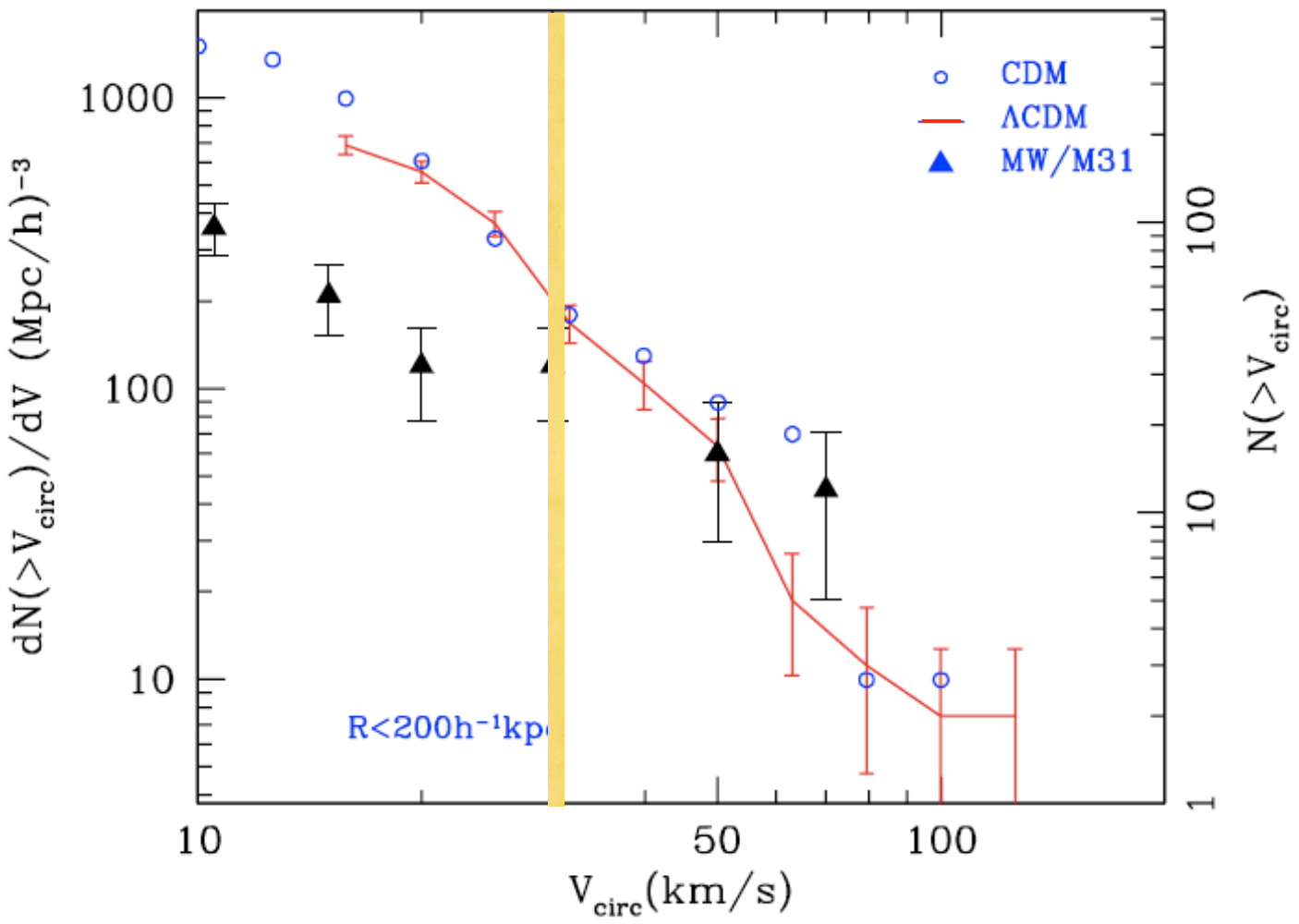
LCDM simulation



Andrey Kravtsov

Local Group





Does CDM  
Predict  
Too Many  
Satellite  
Galaxies?

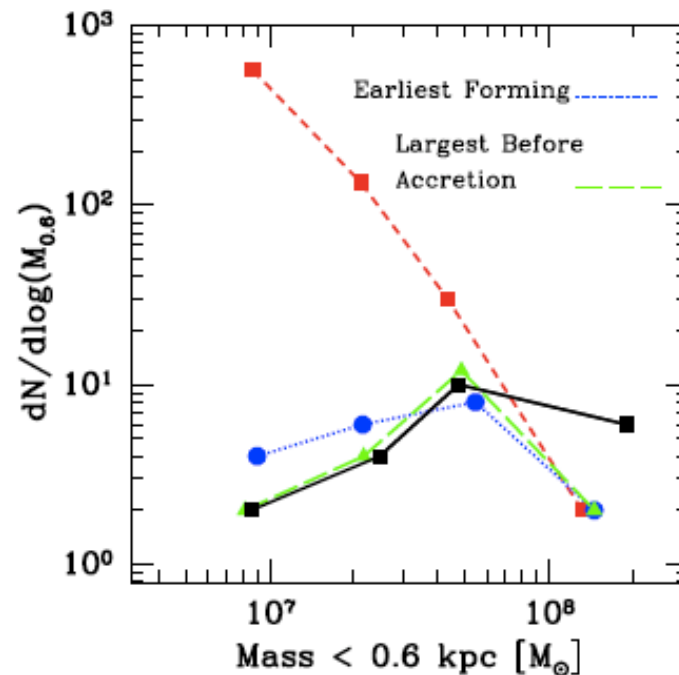
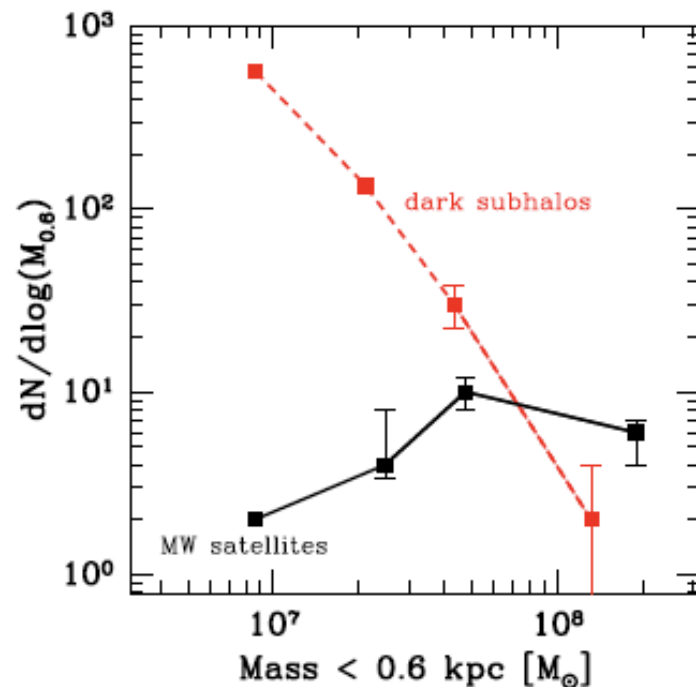
Klypin+1999  
 $\Lambda\text{CDM}$

There are more subhalos with  $V_{\text{circ}} < 30 \text{ km}/\text{s}$  than observed satellites around MW and M31

# Redefining the Missing Satellites Problem

Louis Strigari, James Bullock, Manoj Kaplinghat, Juerg Diemand,  
Michael Kuhlen, & Piero Madau, *ApJ*, 669, 676 (2007)

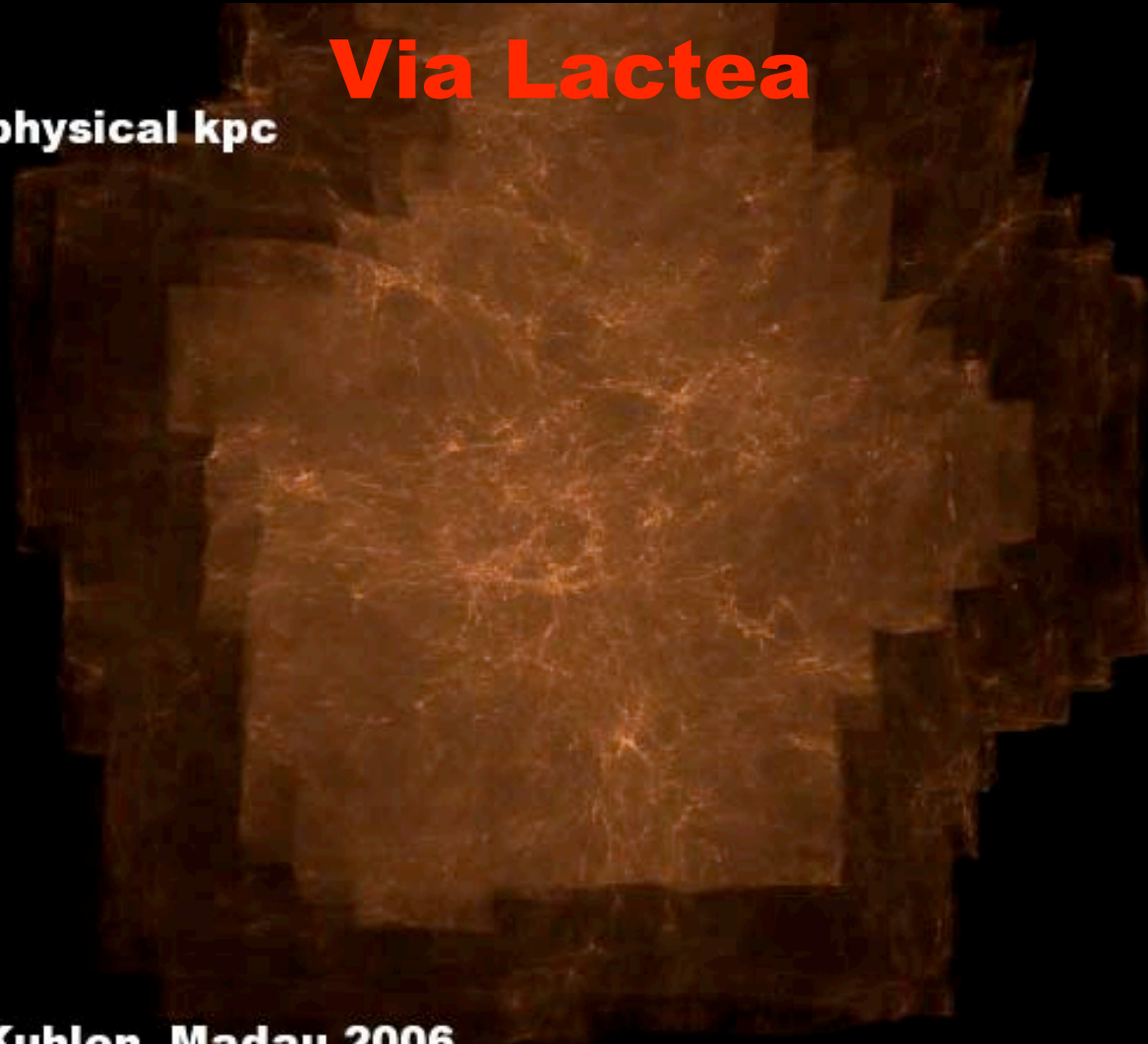
We present comprehensive mass models for the well-known Milky Way dwarf satellites, and derive likelihood functions to show that their masses within 0.6 kpc ( $M_{0.6}$ ) are strongly constrained by the present data. We show that the  $M_{0.6}$  mass function of luminous satellite halos is flat between  $\sim 10^7$  and  $10^8 M_{\odot}$ . We use the **Via Lactea** N-body simulation to show that the  $M_{0.6}$  mass function of CDM subhalos is steeply rising over this range. We rule out the hypothesis that the 11 well-known satellites of the Milky Way are hosted by the 11 most massive subhalos. We show that **models where the brightest satellites correspond to the earliest forming subhalos or the most massive accreted objects** both reproduce the observed mass function.



**z=11.9**

**800 x 600 physical kpc**

# Via Lactea



**Diemand, Kuhlen, Madau 2006**

**Music: Bach Cantata #22**

# The Kinematics of the Ultra-Faint Milky Way Satellites: Solving the Missing Satellite Problem

Joshua Simon & Marla Geha, ApJ 670, 313 (2007)

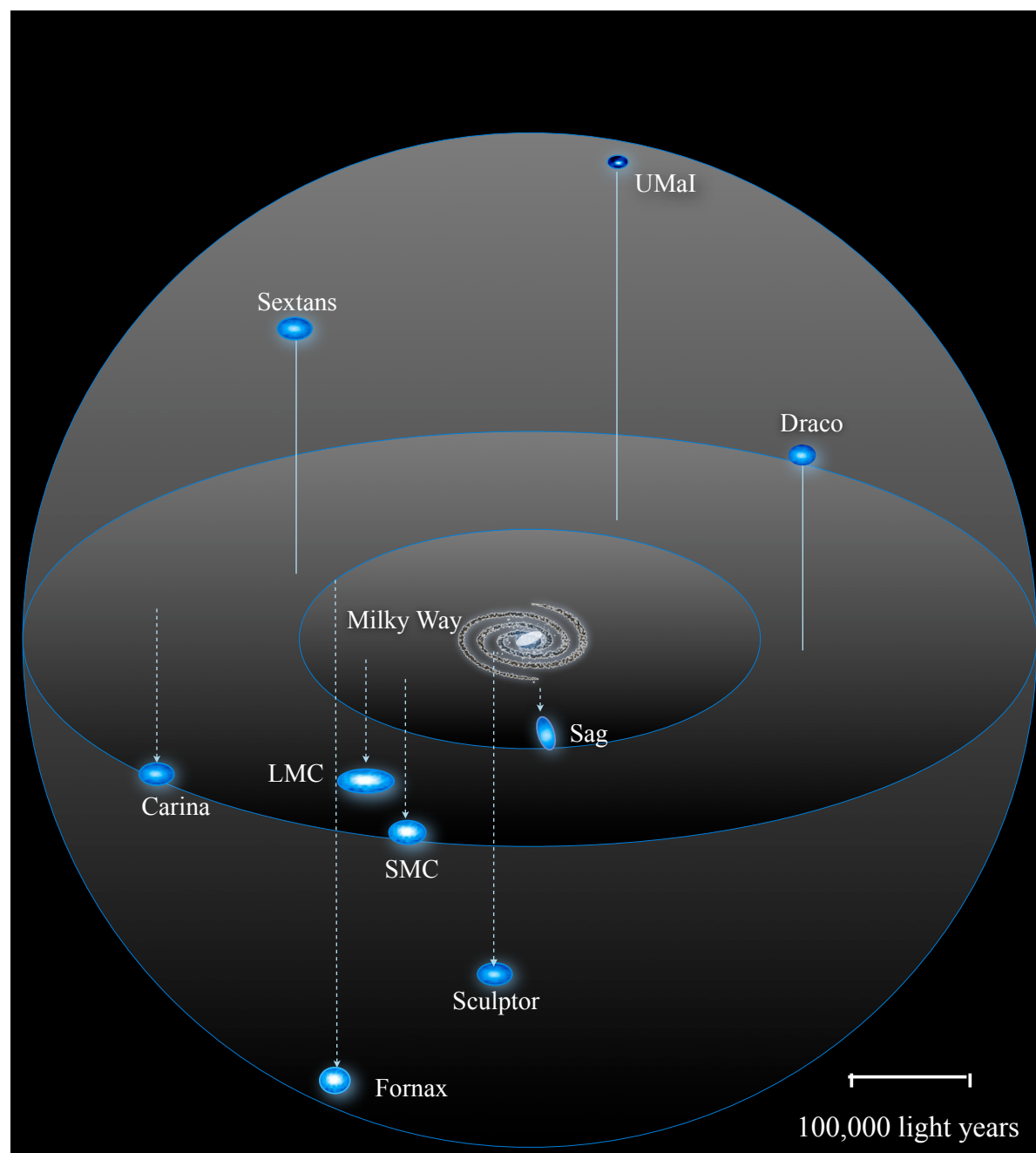
Our understanding of the missing satellite problem and the evolution of dwarf galaxies is being rapidly revised by the **discovery of a large population of new, very faint Local Group dwarfs** in the Sloan Digital Sky Survey and other wide-field imaging surveys. In the past 3 years, at least 20 of these galaxies have been identified, nearly doubling the previously known population. The new dwarfs include 8 additional Milky Way dwarf spheroidals. Since these were discovered in a survey that covered only about 1/5 of the sky, the presence of about 40 more dwarf spheroidals is suggested. These recently discovered MWy satellites have velocity dispersions  $\sigma = 3.3$  to 7.6 km/s. With Mass/Light ratios approaching  $1000 M_{\odot}/L_{\odot}$ , they are the **darkest known stellar systems** in the universe.



# Milky Way circa 2004

## ~11 Dwarf Satellites

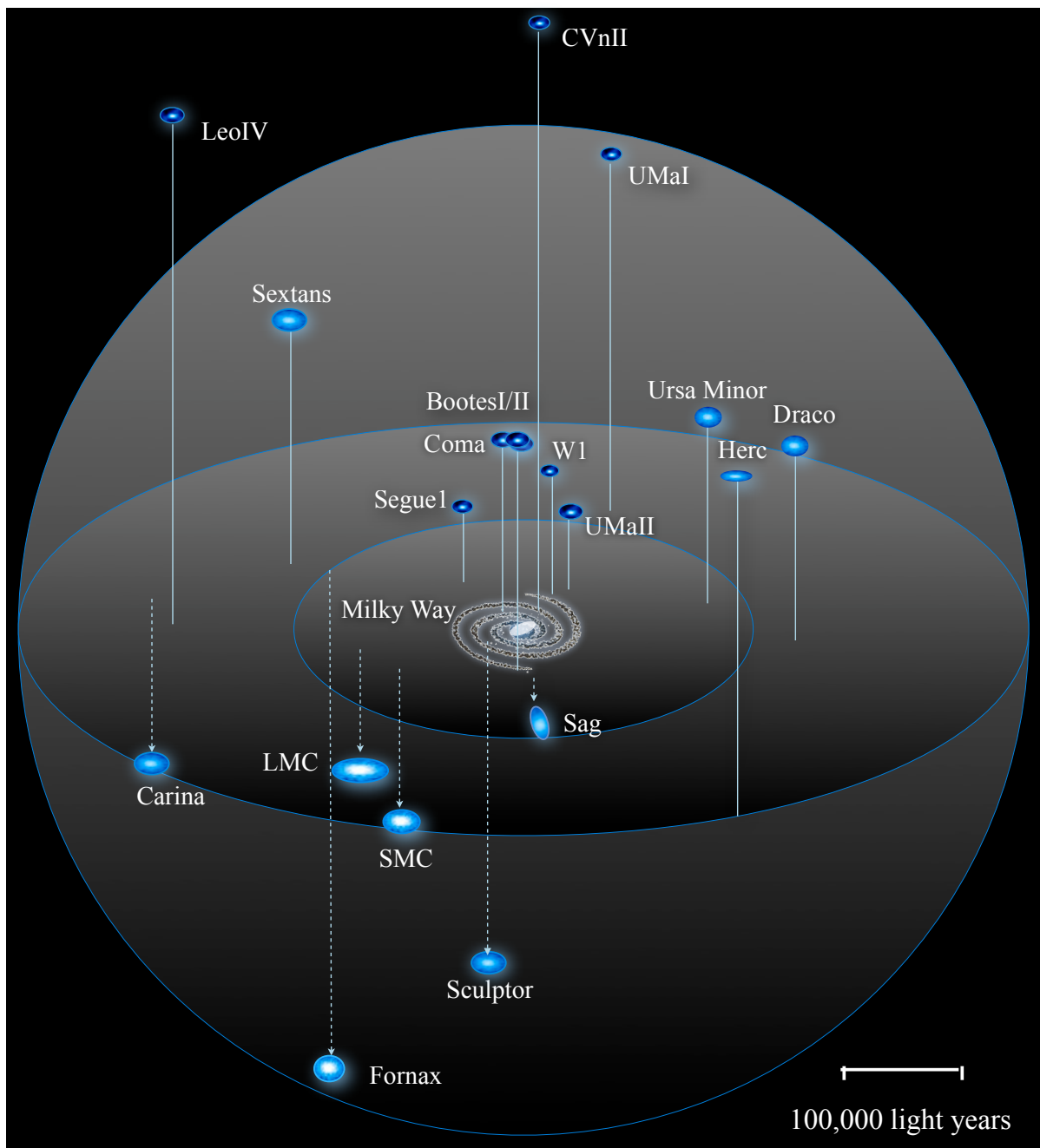
Name	Year Discovered
LMC	1519
SMC	1519
Sculptor	1937
Fornax	1938
Leo II	1950
Leo I	1950
Ursa Minor	1954
Draco	1954
Carina	1977
Sextans	1990
Sagittarius	1994



J. Bullock, UC Irvine

# Milky Way circa 2008

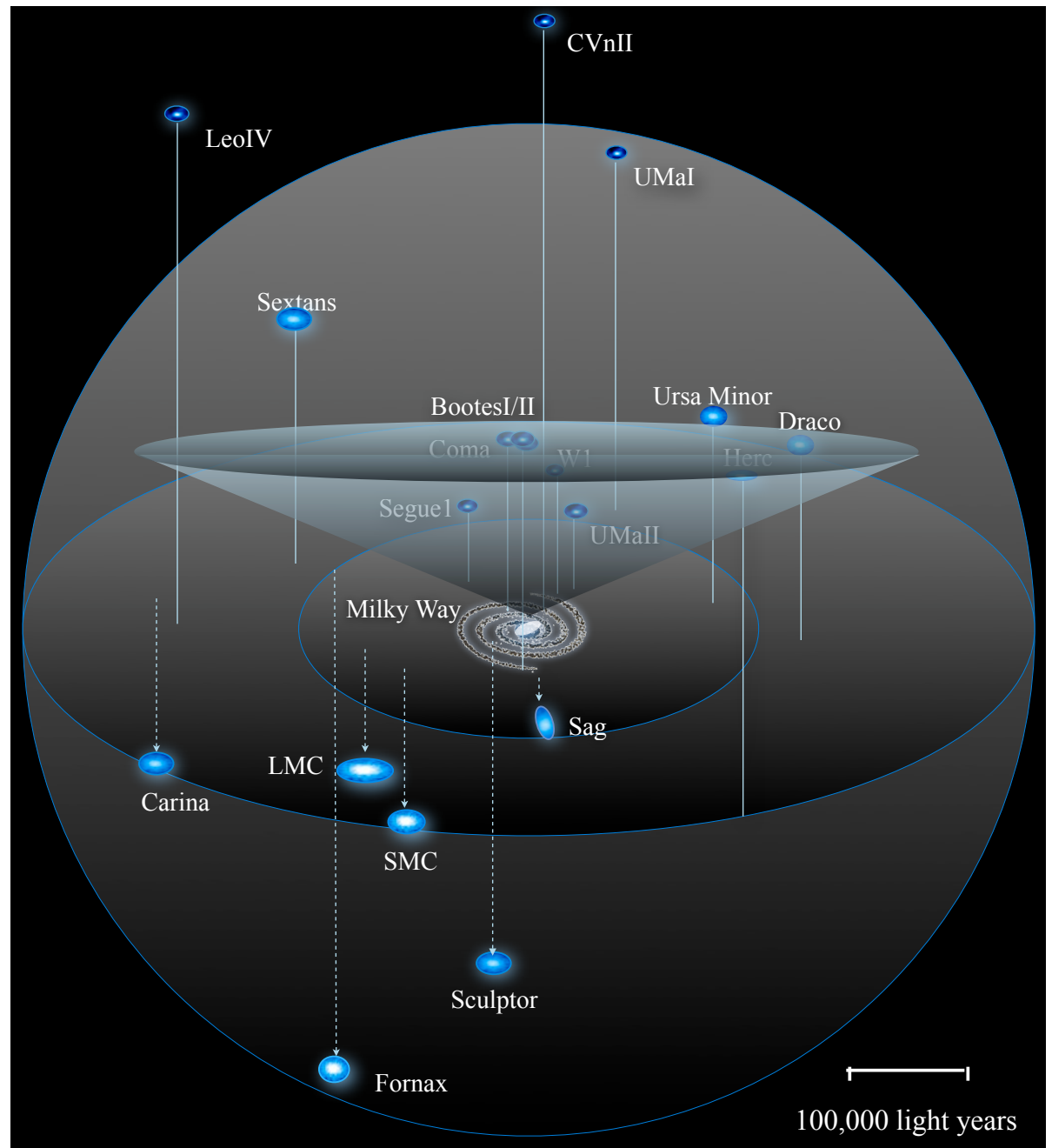
Name	Year Discovered
LMC	1519
SMC	1519
Sculptor	1937
Fornax	1938
Leo II	1950
Leo I	1950
Ursa Minor	1954
Draco	1954
Carina	1977
Sextans	1990
Sagittarius	1994
Ursa Major I	2005
Willman I	2005
Ursa Major II	2006
Bootes	2006
Canes Venatici I	2006
Canes Venatici II	2006
Coma	2006
Segue I	2006
Leo IV	2006
Hercules	2006
Leo T	2007
Bootes II	2007



J. Bullock, UC Irvine

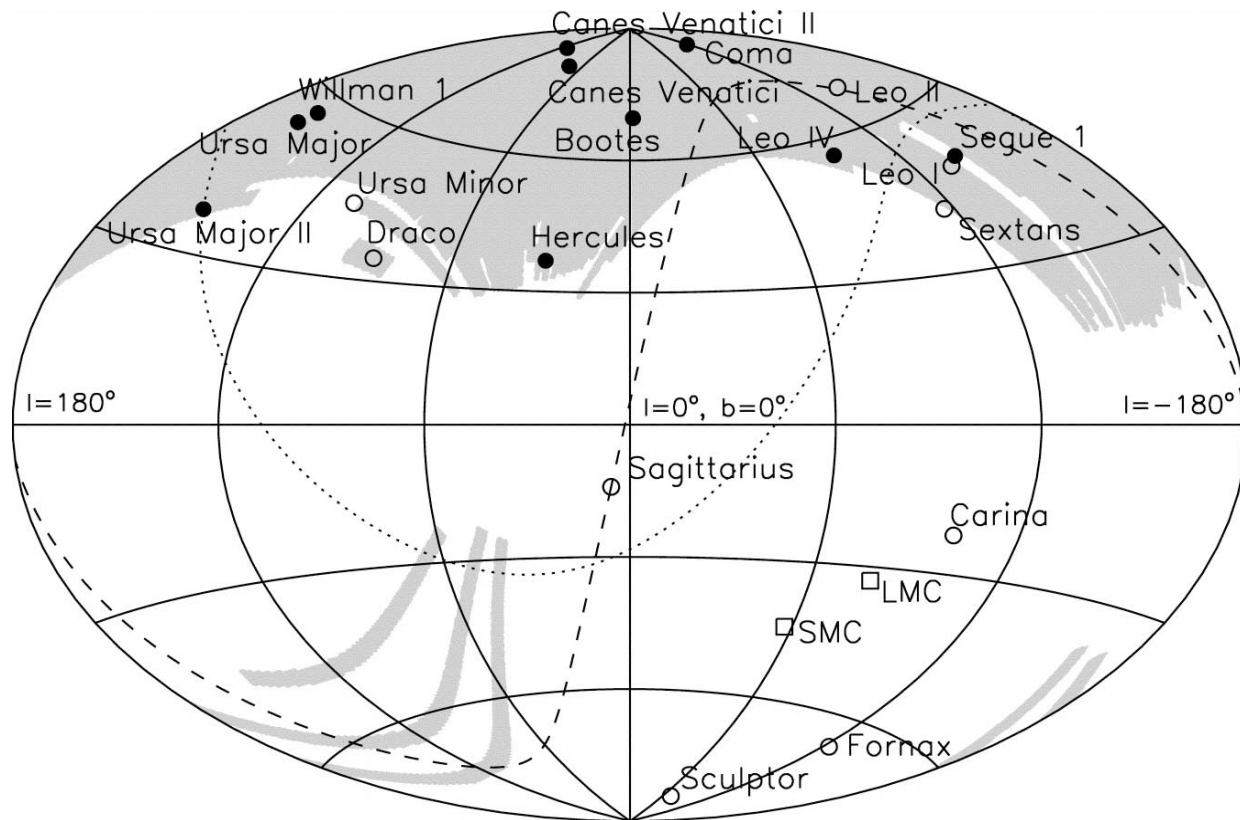
# Milky Way circa 2008

Name	Year Discovered
LMC	1519
SMC	1519
Sculptor	1937
Fornax	1938
Leo II	1950
Leo I	1950
Ursa Minor	1954
Draco	1954
Carina	1977
Sextans	1990
Sagittarius	1994
Ursa Major I	2005
Willman I	2005
Ursa Major II	2006
Bootes	2006
Canes Venatici I	2006
Canes Venatici II	2006
Coma	2006
Segue I	2006
Leo IV	2006
Hercules	2006
Leo T	2007
Bootes II	2007



J. Bullock, UC Irvine

# Many more to be discovered...

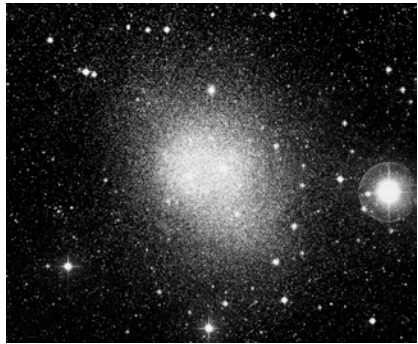


Willman et al.; Zucker et al.; Belokurov et al.; Koposov et al. 07...

**See: Erik Tollerud et al. 2008**

New dwarfs are NOT your old dwarfs...

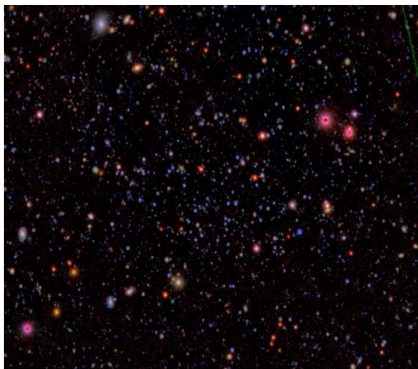
Fornax



$L \sim 10^7 L_{\text{sun}}$

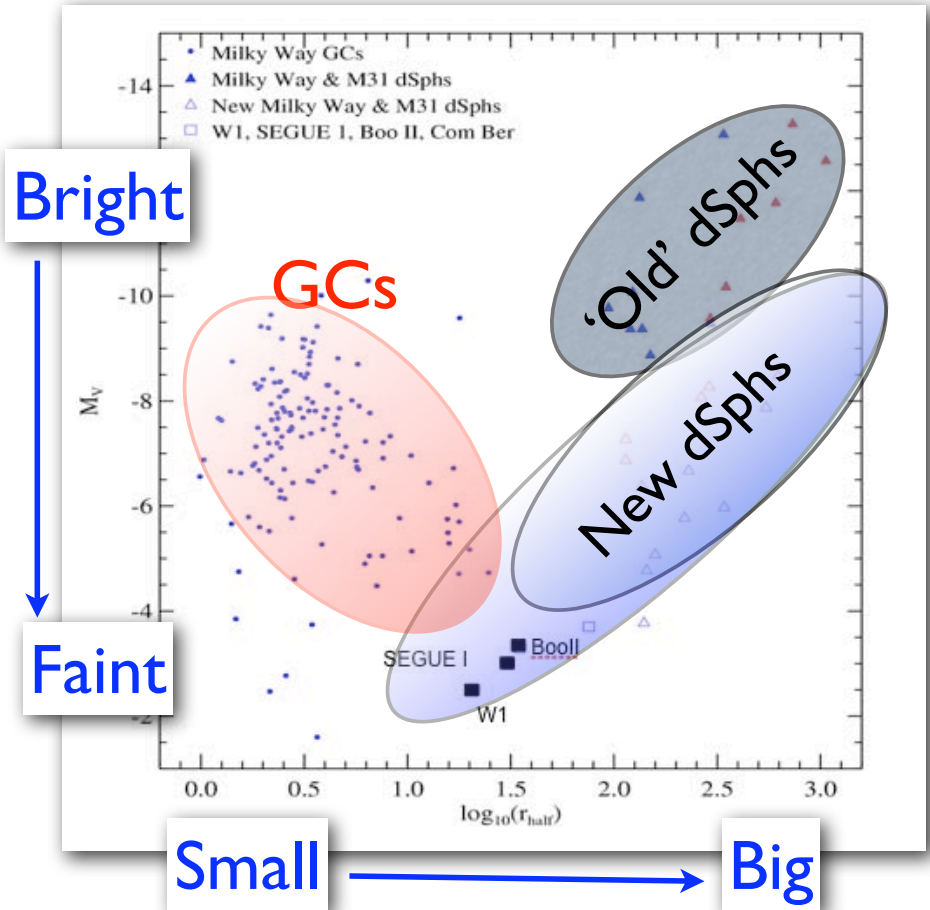
$\sim 3000 \text{ pc}$

Will I



$L \sim 10^3 L_{\text{sun}}$

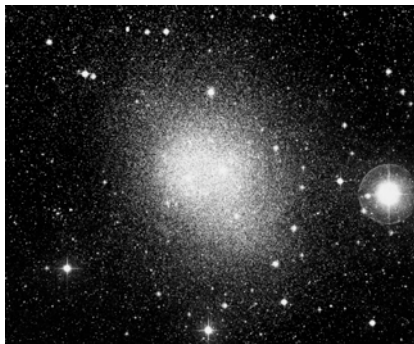
$\sim 80 \text{ pc}$



Compilation by Beth Willman.

# New dwarfs are NOT your old dwarfs...

Fornax

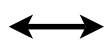


$L \sim 10^7 L_{\text{sun}}$



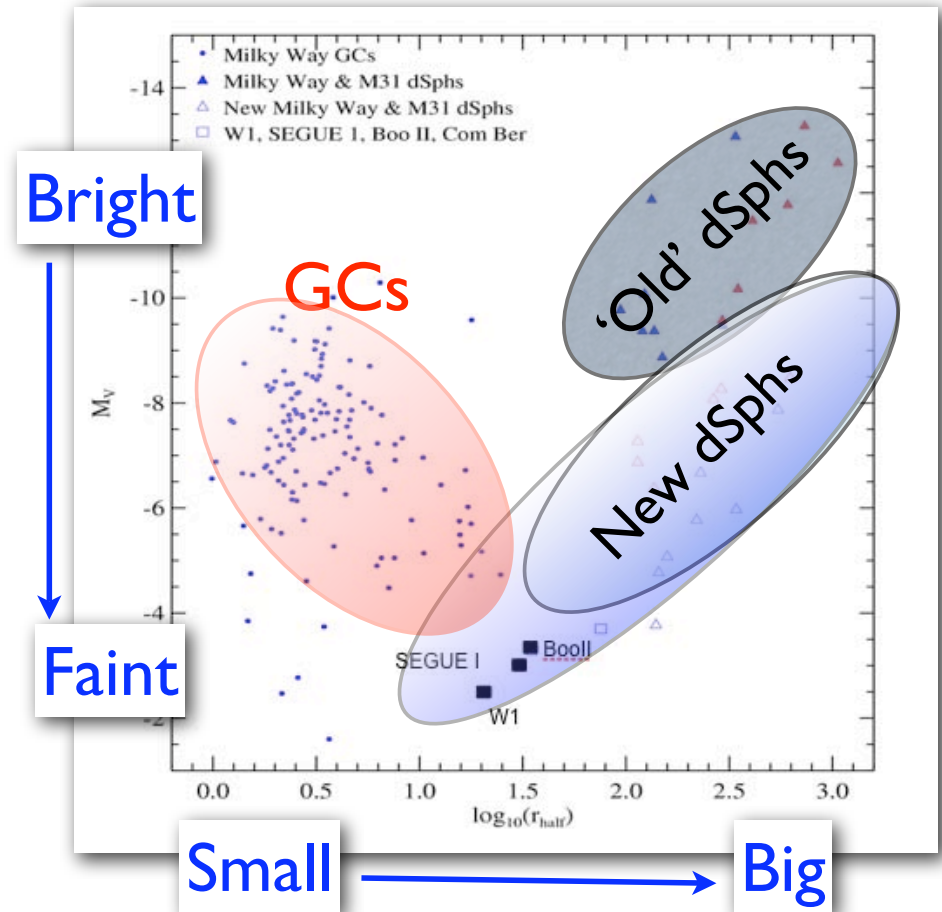
$\sim 3000 \text{ pc}$

Will I



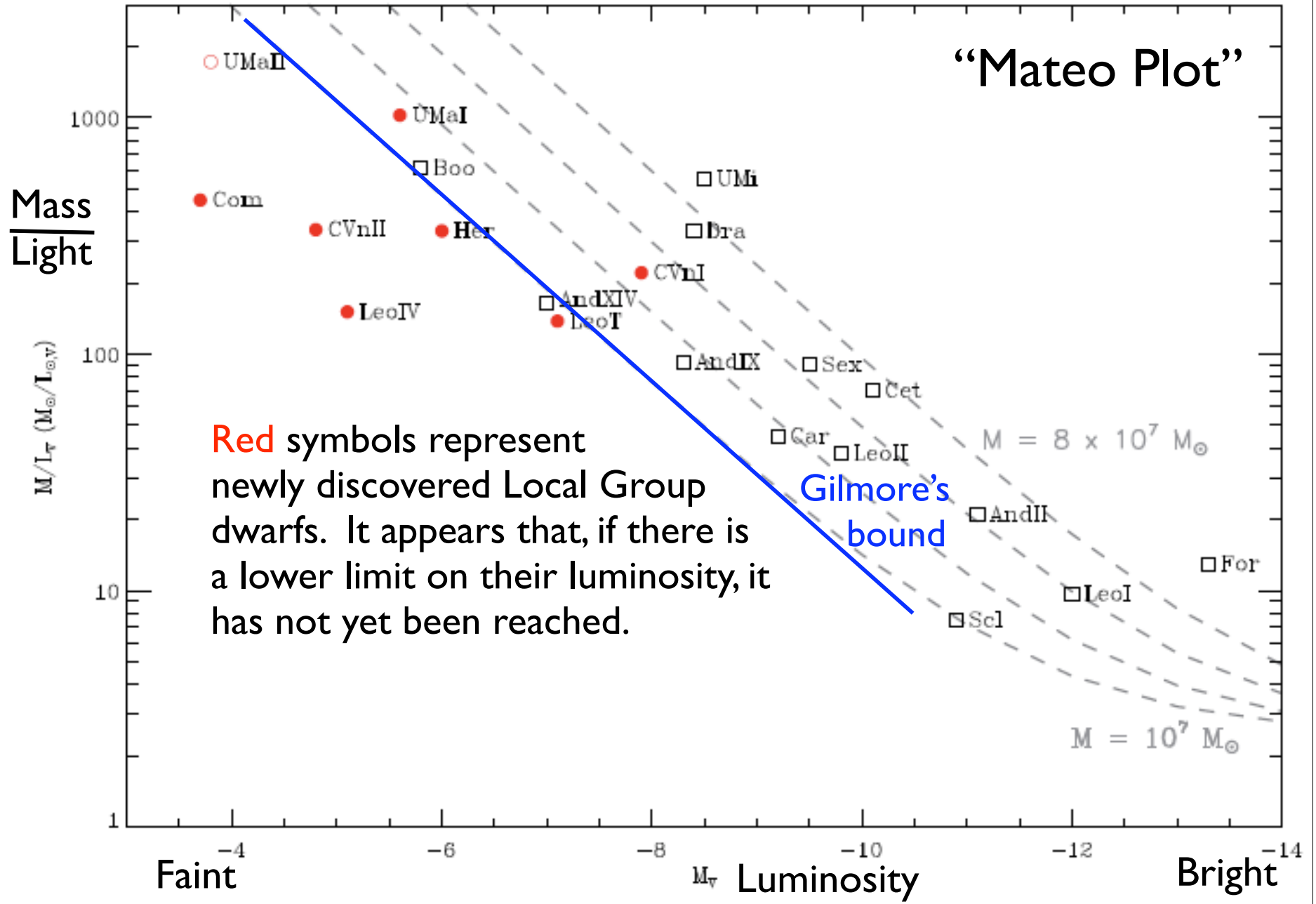
$\sim 80 \text{ pc}$

$L \sim 10^3 L_{\text{sun}}$

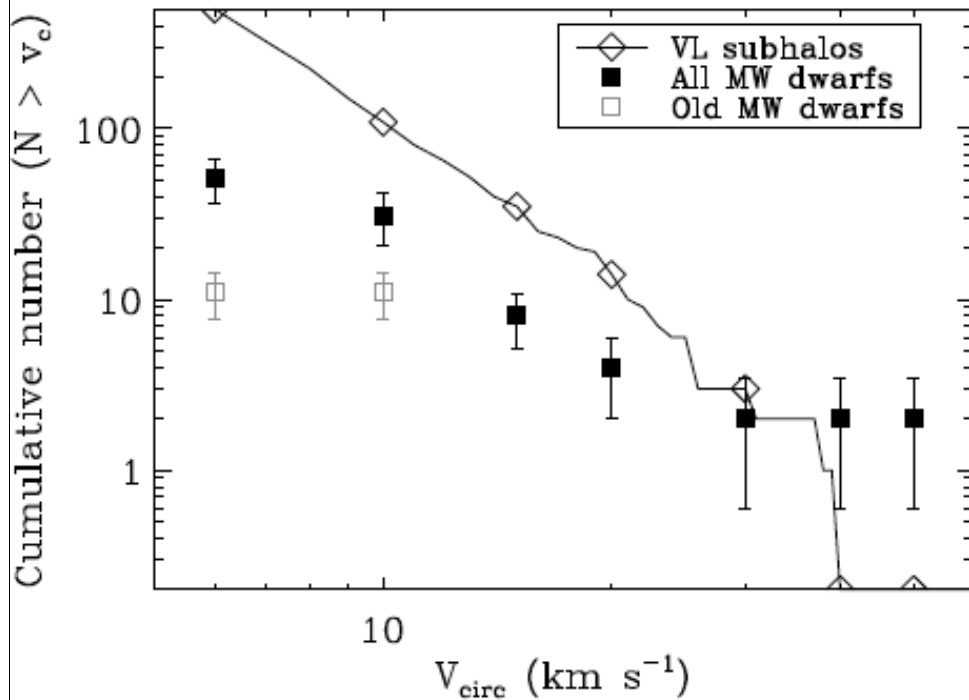


Compilation by Beth Willman.

# “Mateo Plot”

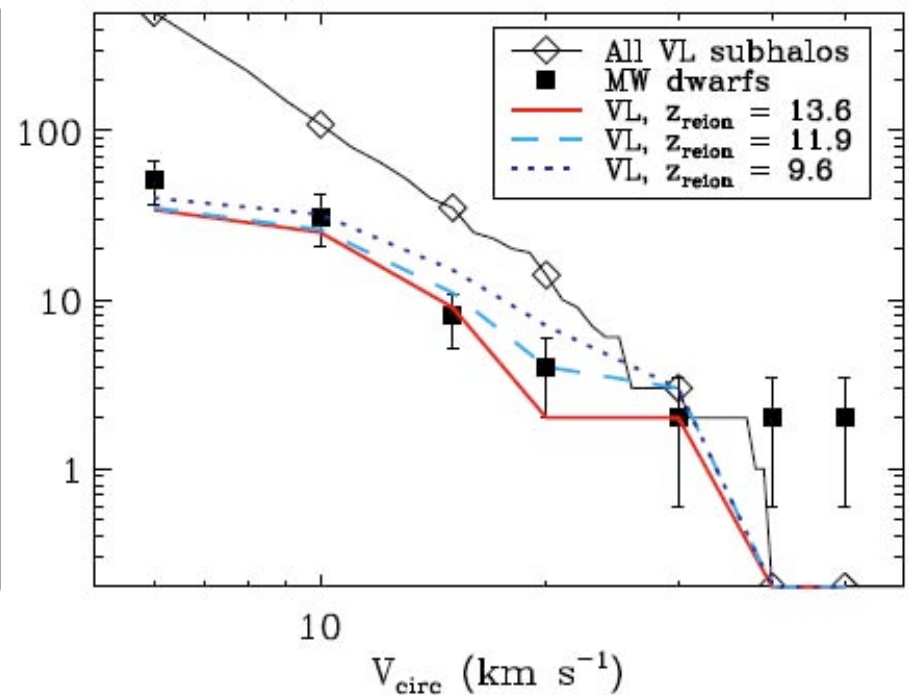


Simon & Geha, ApJ 670, 313 (2007)



Cumulative number of Milky Way satellite galaxies as a function of halo circular velocity, assuming Poisson errors on the number count of satellites in each bin (computed independently for the new and old dwarfs). The filled black squares include the new circular velocity estimates from Simon & Geha 2007, who follow Klypin+1999 and use  $V_{\text{circ}} = \sqrt{3} \sigma$ . Diamonds represent all subhalos within the virial radius in the Via Lactea simulation (Diemand+2007).

[Simon & Geha, ApJ 670, 313 \(2007\)](#)



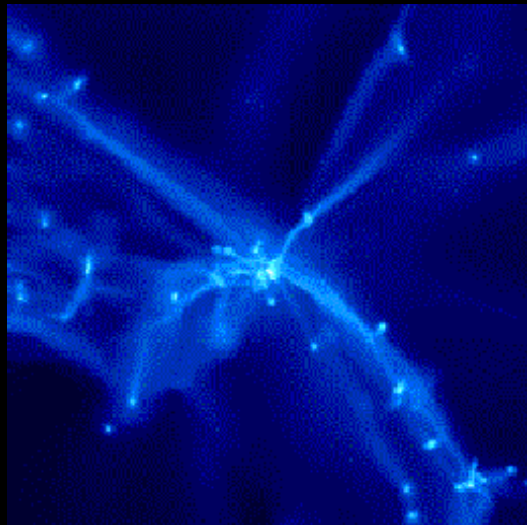
Effect of reionization on the missing satellite problem. The solid red curve shows the circular velocity distribution for the 51 most massive Via Lactea subhalos at  $z = 13.6$ , the dashed cyan curve at  $z = 11.9$ , and the dotted blue curve at  $z = 9.6$ . Thus, [suppression of star formation in small dwarfs after reionization can account for the observed satellites in  \$\Lambda\$ CDM](#), as suggested by Bullock+2000, Somerville 2002, Benson+2003, and Moore+2006.



Does this mean that the “Too Many Subhalos” problem has been solved? Not quite...

- the details of “squelching” of star formation in dwarfs need to be worked out and compared to the new data
- the more reliable  $M_{0.6}$  method of Strigari+2007 has been applied to the newly discovered Local Group satellite galaxies, implies they have common mass
- simulations must have converged in resolving all relevant subhalos

# Modeling of dwarfs



## 1. N-body (DM only) Simulations

- ◆ solve equations of gravity for particles of dark matter (& sometimes stars)

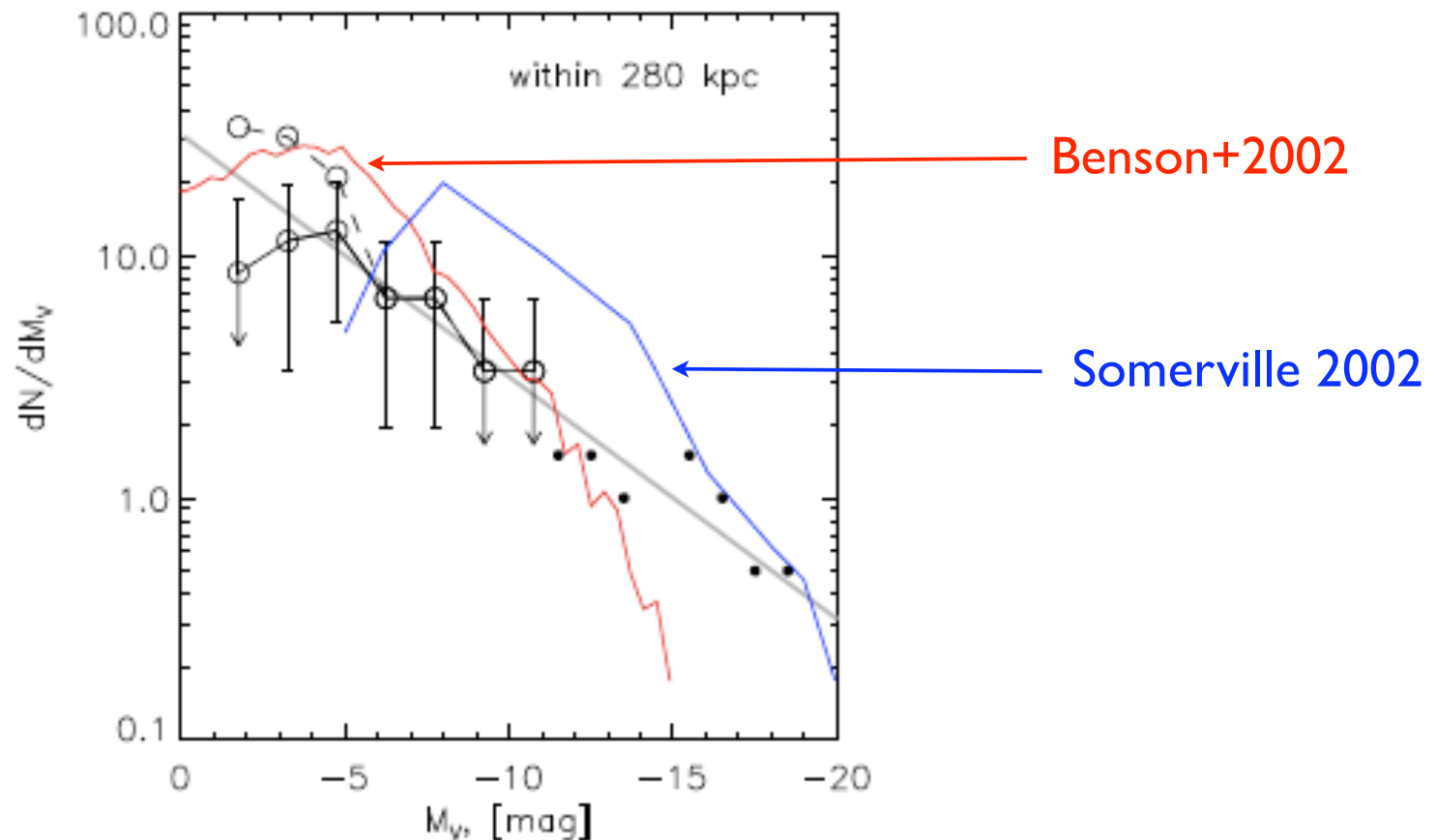
## 2. Hydrodynamic Simulations

- ◆ solve equations of gravity and hydrodynamics/thermodynamics for particles of dark matter and gas

## 3. Semi-Analytic Models

- ◆ treat gravity and “gastrophysics” via analytic approximations based on 1 & 2

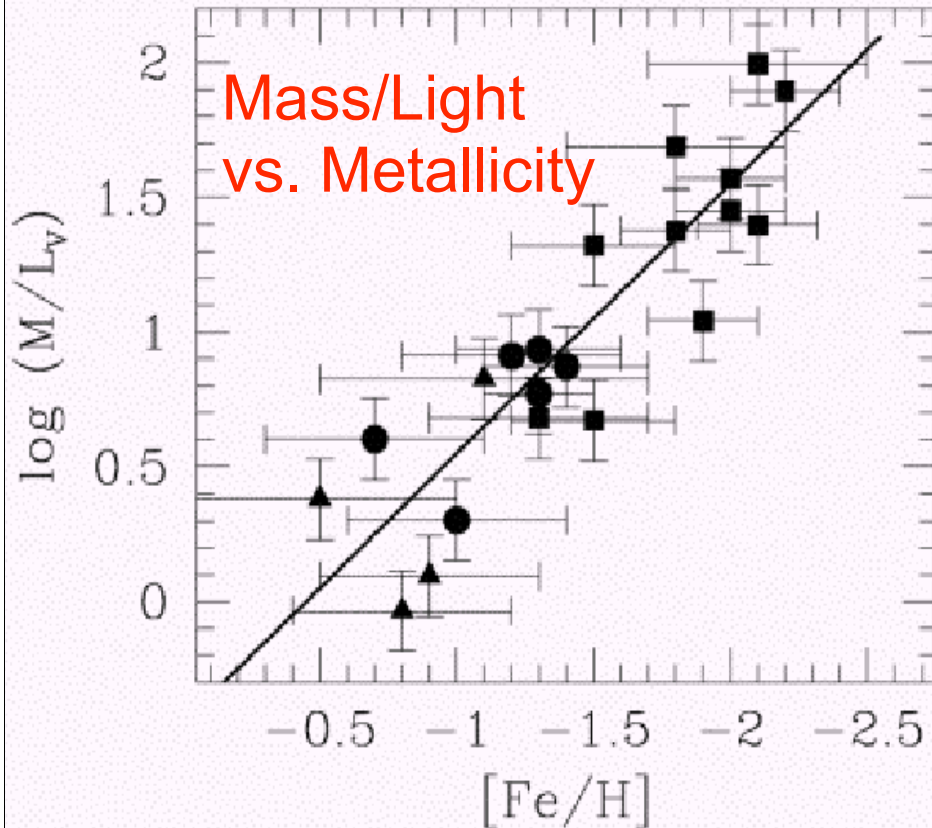
# Luminosity Function of the Local Group: SDSS Data Compared with Semi-Analytic Models



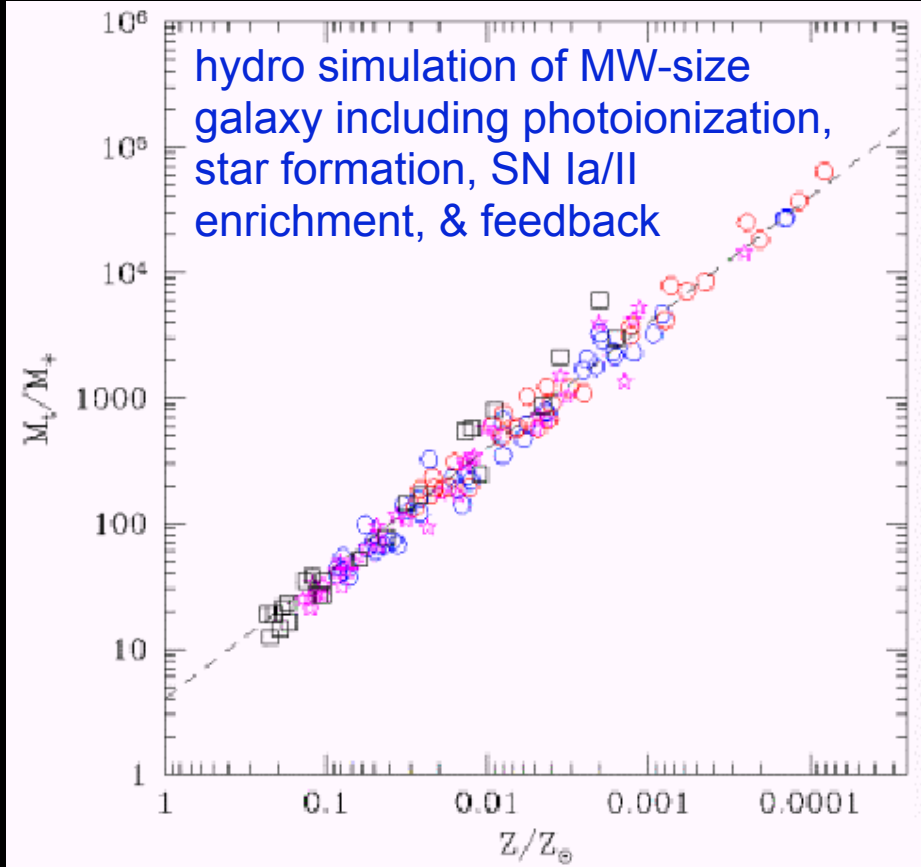
The models include reionization, feedback, and (for Benson+) tidal stripping. Neither model agrees perfectly with the data.

This figure is from Kopolov, Belokurov, + [arXiv0706.2687](https://arxiv.org/abs/0706.2687).

# Challenge to explain other properties of LG dwarfs



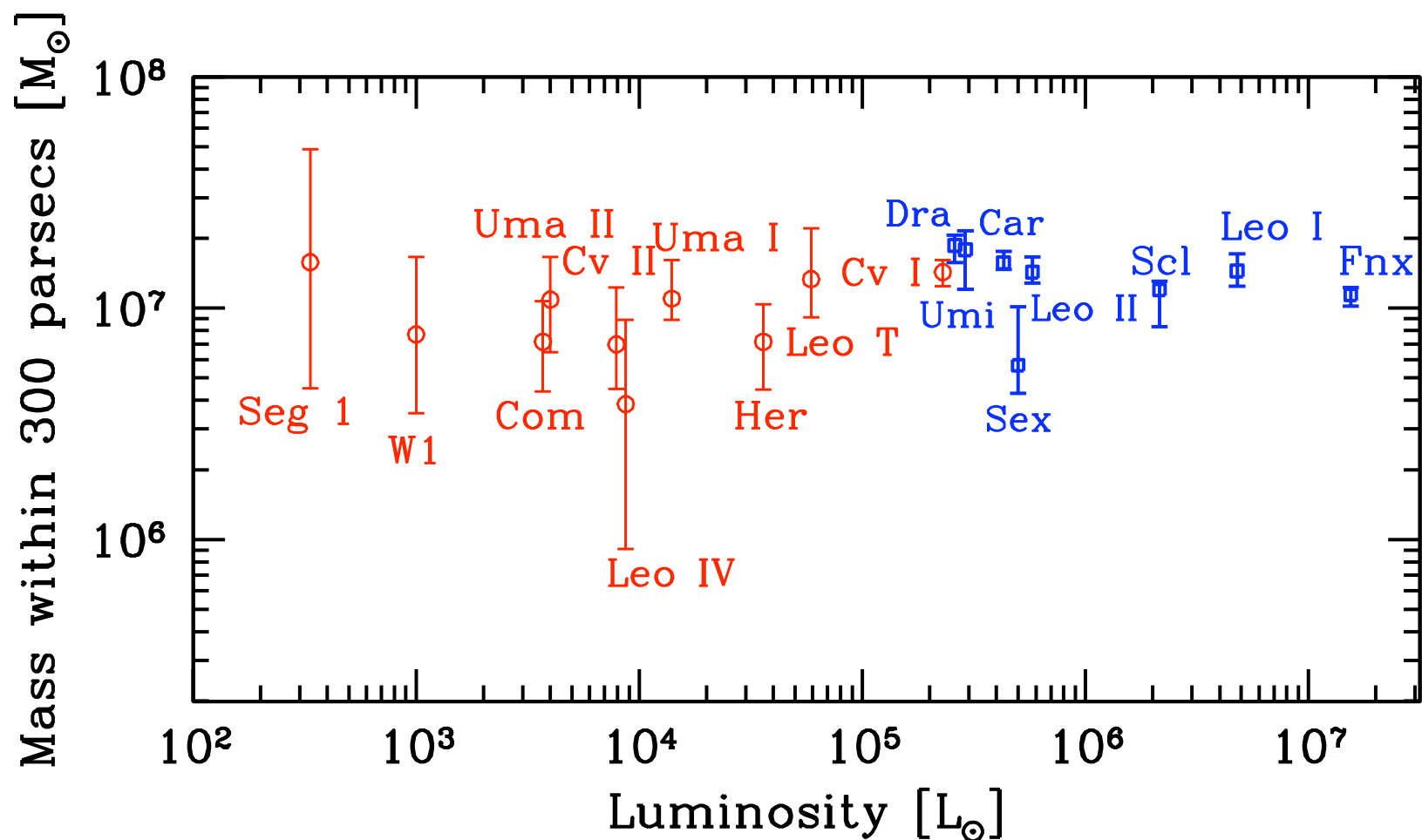
Prada & Burkert 2002; cf. Dekel & Woo 2003



Andrey Kravtsov 2003

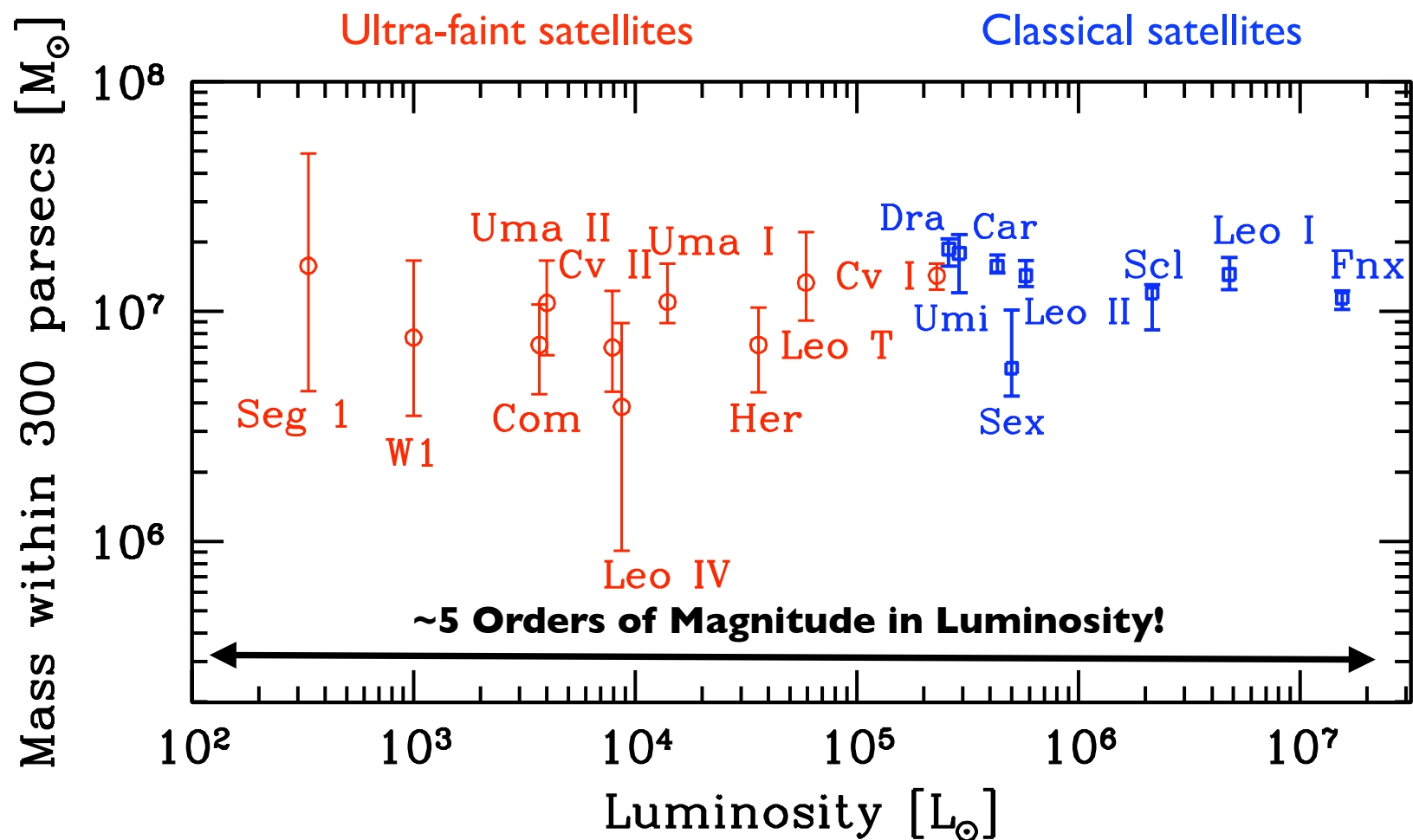
Note: feedback may not be essential (Simon+06)

# A Common Mass for MW Satellite Galaxies



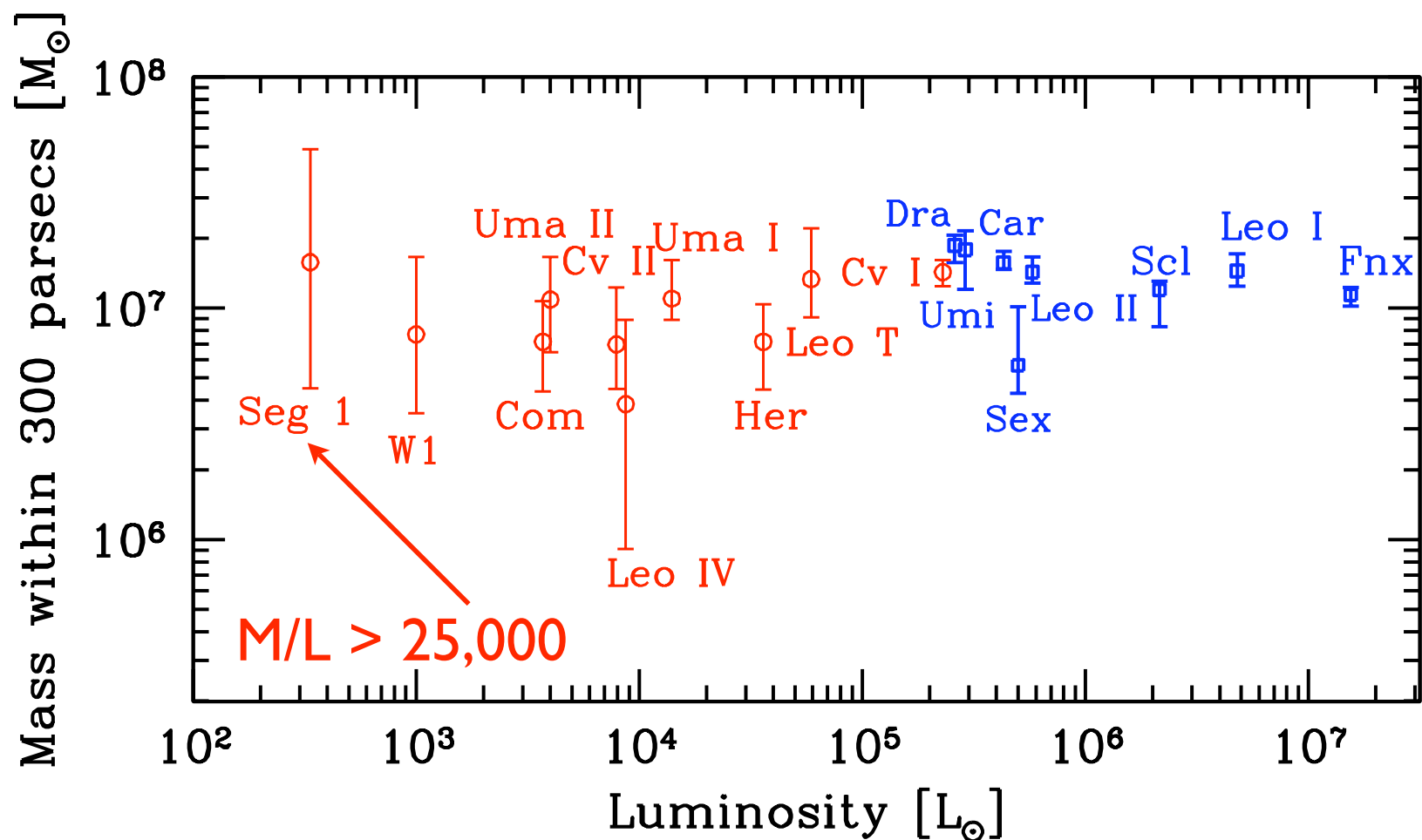
L. Strigari, J. Bullock, M. Kaplinghat, J. Simon, M. Geha, B. Willman, M. Walker,  
[Nature, Aug 28, 2008]

# A Common Mass for MW Satellite Galaxies



L. Strigari, J. Bullock, M. Kaplinghat, J. Simon, M. Geha, B. Willman, M. Walker,  
[Nature, Aug 28, 2008]

# A Common Mass for MW Satellite Galaxies

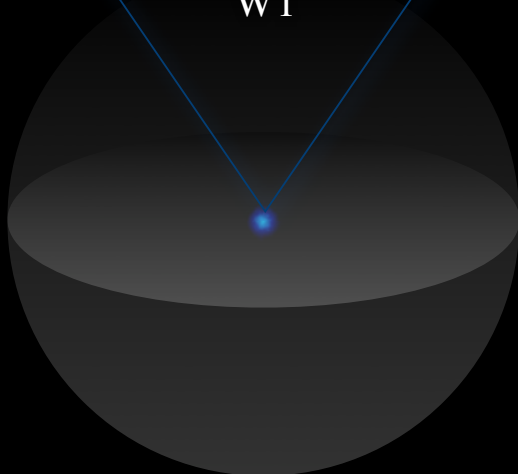


L. Strigari, J. Bullock, M. Kaplinghat, J. Simon, M. Geha, B. Willman, M. Walker,  
[Nature, Aug 28, 2008]

$L = 10^3 L_{\text{sun}}$   
100 pc



W1



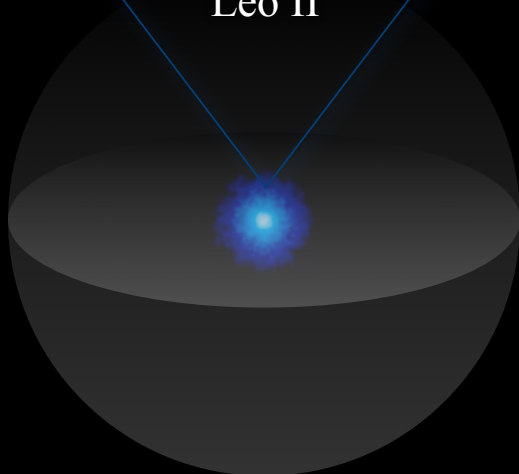
$M_{300} = 10^7 M_{\text{sun}}$

$M_{\text{vir}} \sim 10^9 M_{\text{sun}}$

$L = 5 \cdot 10^5 L_{\text{sun}}$   
500 pc



Leo II



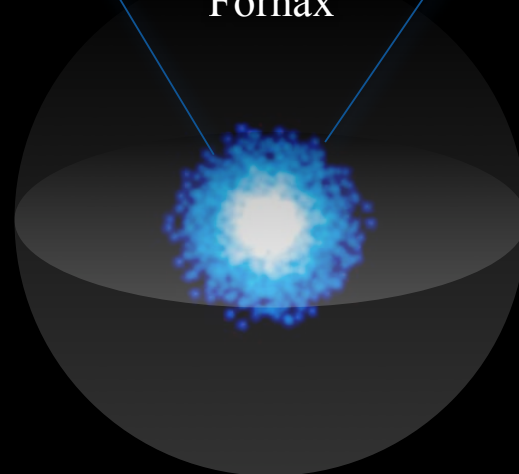
$M_{300} = 10^7 M_{\text{sun}}$

$M_{\text{vir}} \sim 10^9 M_{\text{sun}}$

$L = 10^7 L_{\text{sun}}$   
2000 pc



Fornax

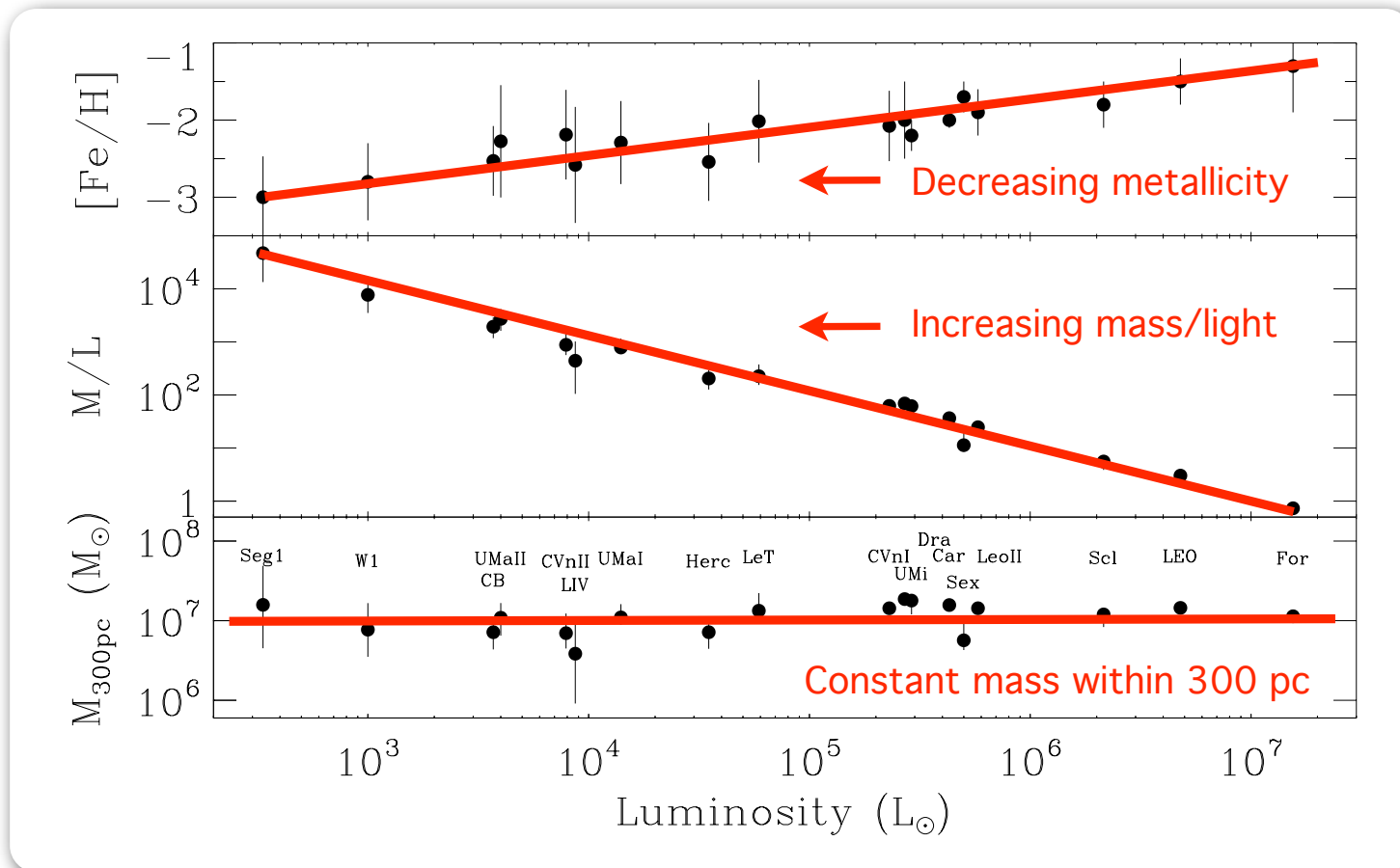


$M_{300} = 10^7 M_{\text{sun}}$

$M_{\text{vir}} \sim 10^9 M_{\text{sun}}$

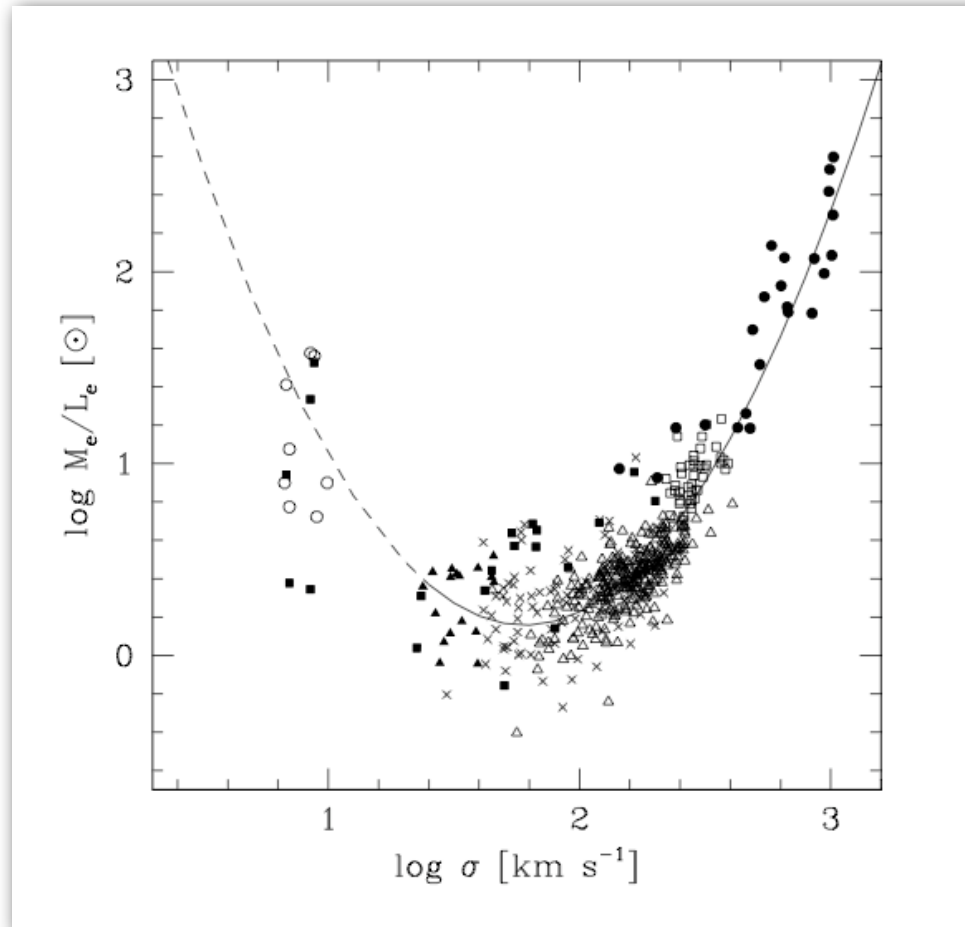


# Kirby et al 2008; Geha et al. 2008



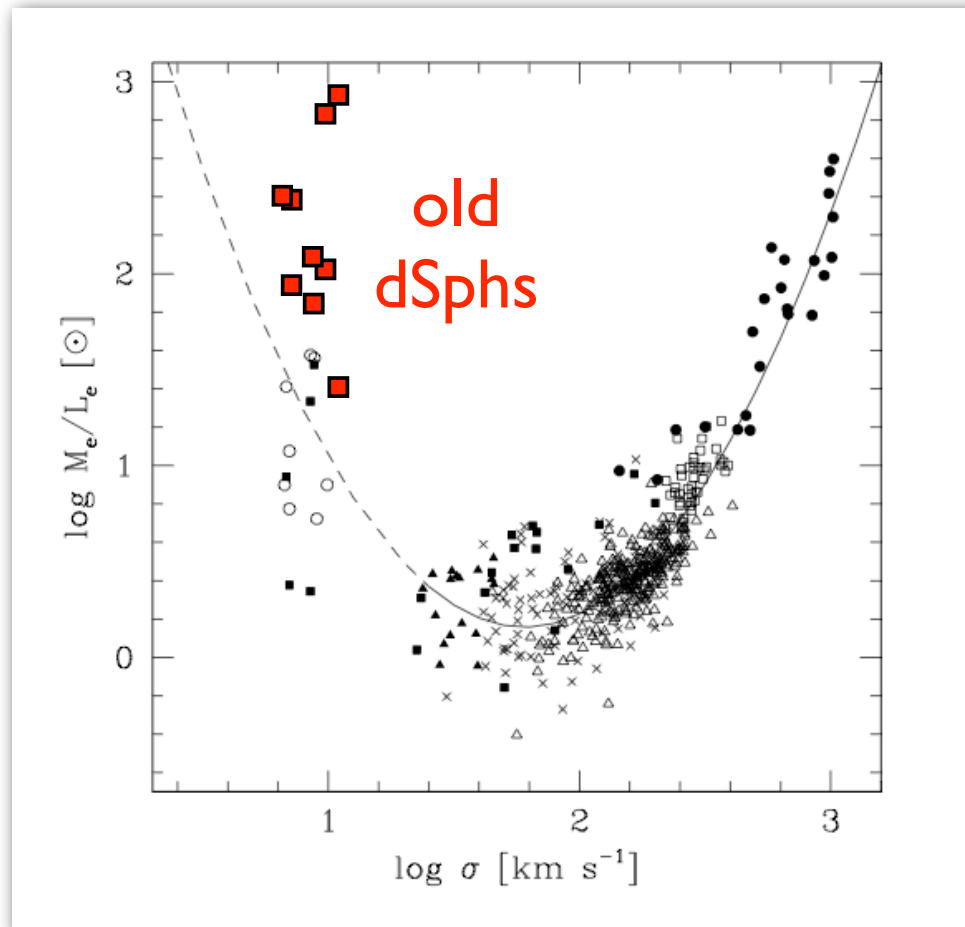
**Metallicity-Luminosity Relationship NOT set by potential well depth!**

## Implications for galaxy formation?



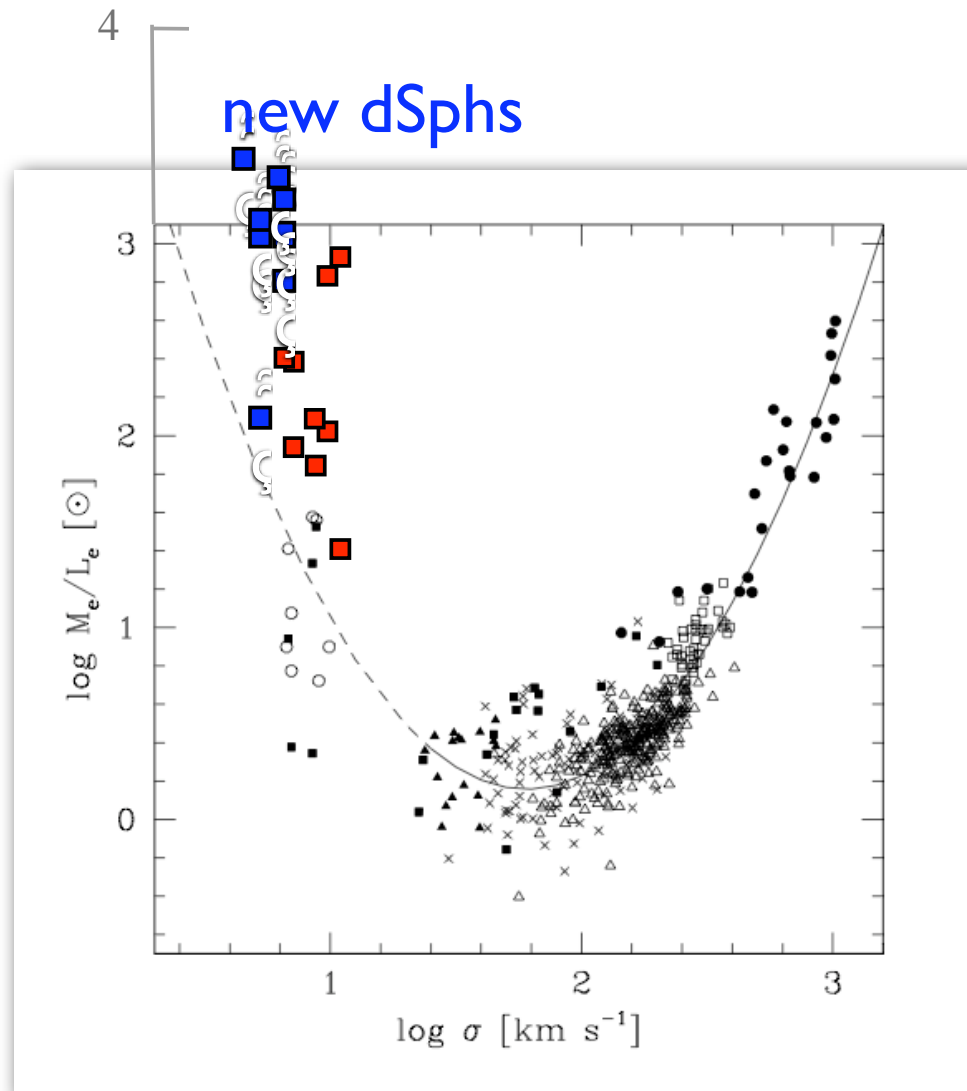
Zaritsky, Gonzalez, & Zabludoff 06

## Implications for galaxy formation?



Zaritsky, Gonzalez, & Zabludoff 06

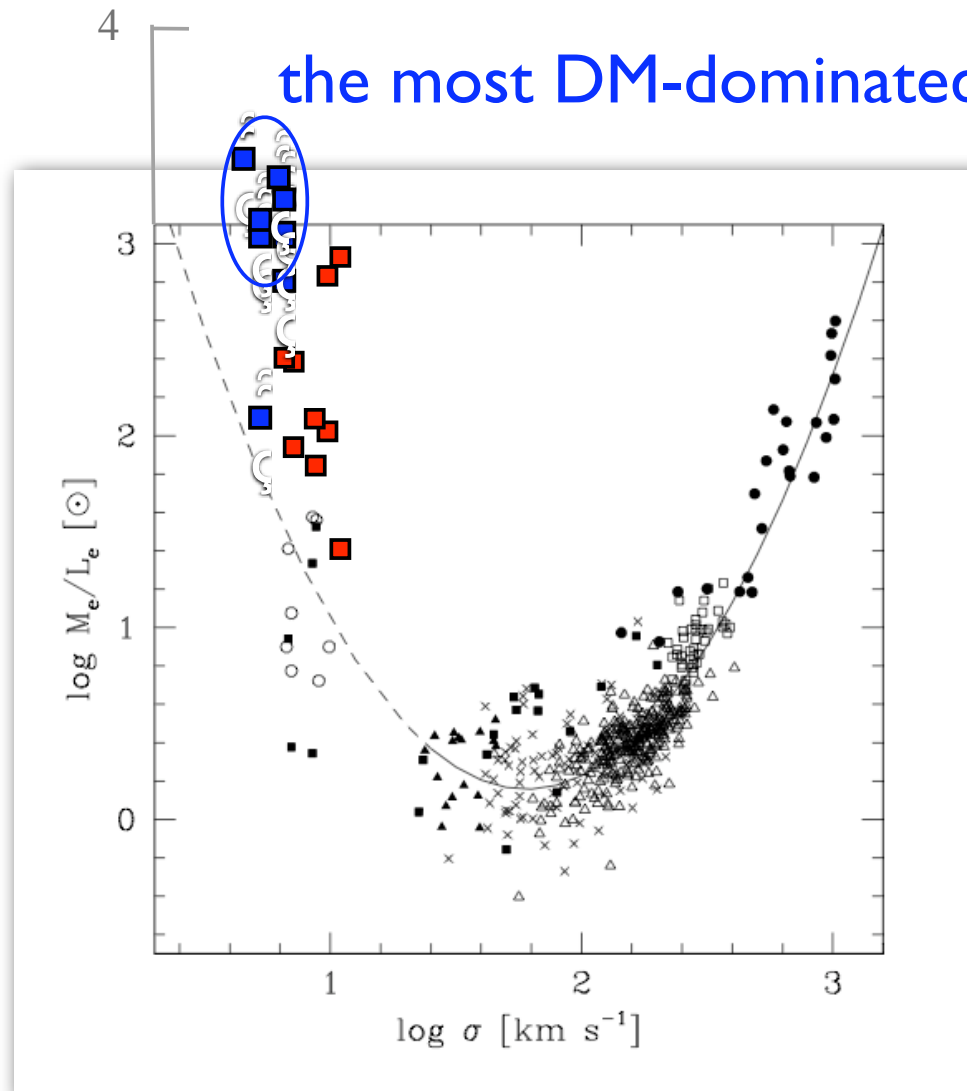
## Implications for galaxy formation?



Zaritsky, Gonzalez, & Zabludoff 06

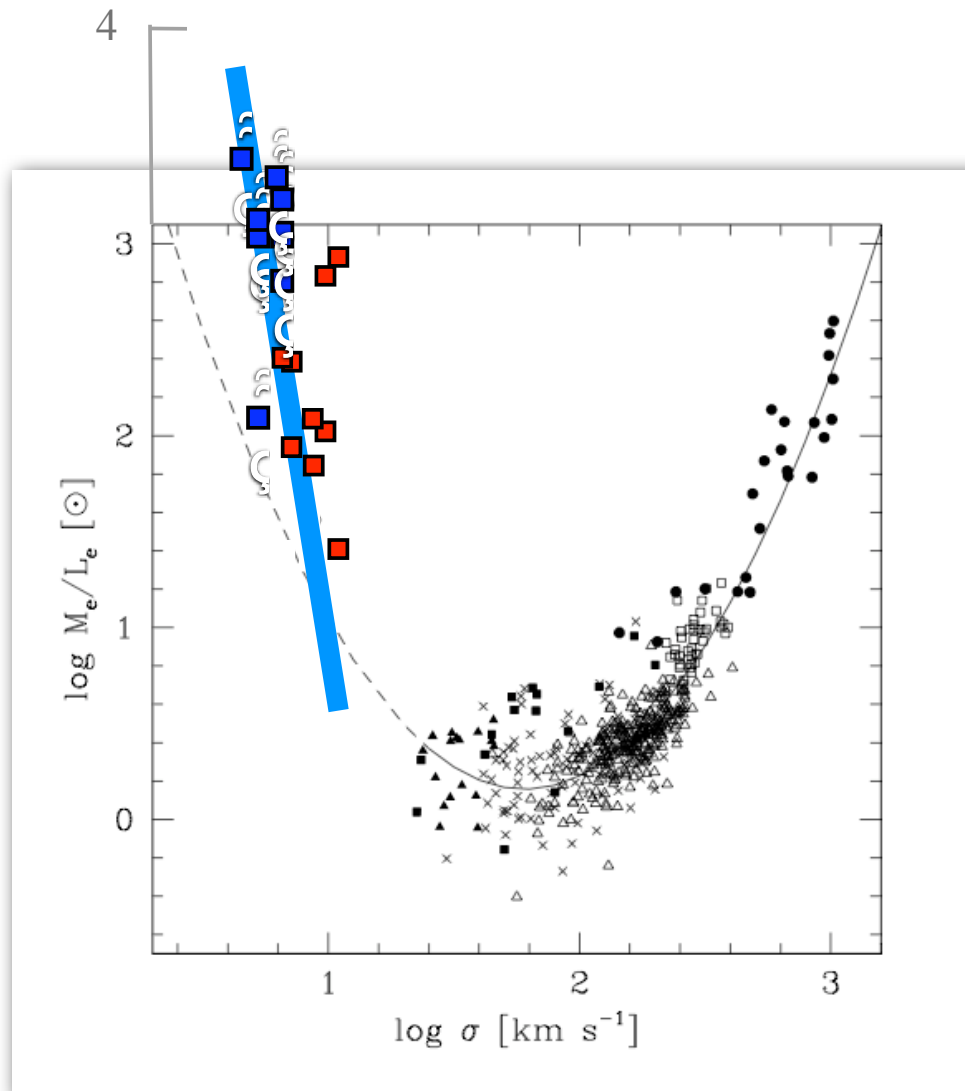
## Implications for galaxy formation?

the most DM-dominated objects known



Zaritsky, Gonzalez, & Zabludoff 06

## Implications for galaxy formation?



Zaritsky, Gonzalez, & Zabludoff 06

## Does this mean that the “Too Many Subhalos” problem has been solved? Not quite...

- the details of “squelching” of star formation in dwarfs need to be worked out and compared to the new data
- the more reliable  $M_{0.6}$  method of Strigari+2007 has been applied to the newly discovered Local Group satellite galaxies, implies they have common mass
- simulations must have converged in resolving all relevant subhalos

## Does this mean that the “Too Many Subhalos” problem has been solved? Not quite...

- the details of “squelching” of star formation in dwarfs need to be worked out and compared to the new data
- the more reliable  $M_{0.6}$  method of Strigari+2007 has been applied to the newly discovered Local Group satellite galaxies, implies they have common mass
- simulations must have converged in resolving all relevant subhalos **Via Lactea II resolves to  $\sim 10$  kpc**



# Via Lactea II

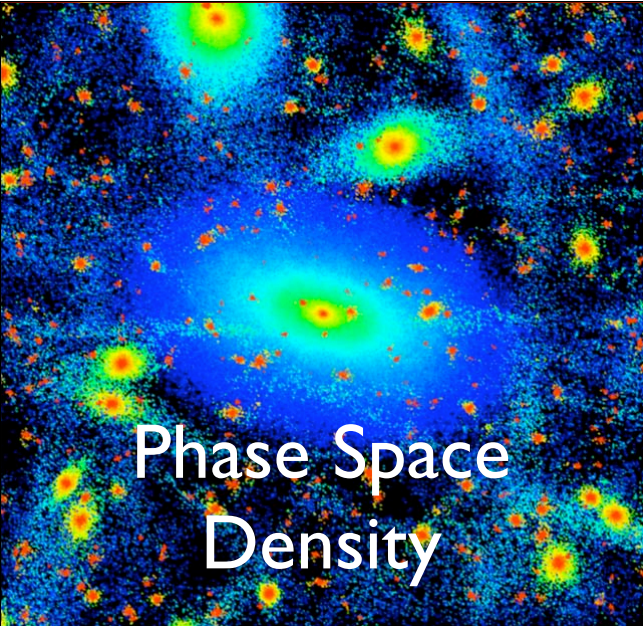
WMAP3 parameters

>  $10^9$  particles

>  $10^6$  cpu hours

Cray XT3 "Jaguar"

ORNL



Phase Space  
Density

A phase space density plot showing a distribution of particles in a 6D phase space. The plot is color-coded, with blue representing lower density and yellow/red representing higher density. Several distinct clumps or structures are visible against a noisy background.



40 kpc

Density<sup>2</sup>



Density

A density plot showing a large, diffuse, elliptical structure. The center is the most dense, shown in red, transitioning through yellow and green to blue at the edges. The background is dark blue with scattered small particles.

J. Diemand,  
M. Kuhlen,  
P. Madau,  
M. Zemp,  
B. Moore,  
D. Potter,  
& J. Stadel

# $\Lambda$ CDM May Be Able To Explain the Observed Gravitational Lensing Flux Anomalies

The fraction of mass in **Via Lactea II** subhalos of mass  $\sim 10^6 - 10^8 M_{\odot}$  is  $\sim 0.5\%$ . This is about the amount needed to explain the flux anomalies observed in radio images of quasars that are quadruply gravitationally lensed by foreground elliptical galaxies (Juerg Diemand and R. Benton Metcalf, private communications). Free streaming of WDM particles can considerably dampen the matter power spectrum in this mass range, so a WDM model with an insufficiently massive particle (sterile neutrino  $m_{\nu} < 10 \text{ keV}$ ) fails to reproduce the observed flux anomalies (Marco Miranda & Andrea Maccio 2007, MNRAS, 382, 1225).

# $\Lambda$ CDM May Be Able To Explain the Observed Gravitational Lensing Flux Anomalies

The fraction of mass in **Via Lactea II** subhalos of mass  $\sim 10^6 - 10^8 M_{\odot}$  is  $\sim 0.5\%$ . This is **about the amount needed to explain the flux anomalies observed in radio images of quasars** that are quadruply gravitationally lensed by foreground elliptical galaxies (Juerg Diemand and R. Benton Metcalf, private communications). Free streaming of WDM particles can considerably dampen the matter power spectrum in this mass range, so a WDM model with an insufficiently massive particle (sterile neutrino  $m_{\nu} < 10 \text{ keV}$ ) fails to reproduce the observed flux anomalies (Marco Miranda & Andrea Maccio 2007, MNRAS, 382, 1225).

# $\Lambda$ CDM May Be Able To Explain the Observed Gravitational Lensing Flux Anomalies

The fraction of mass in **Via Lactea II** subhalos of mass  $\sim 10^6 - 10^8 M_{\odot}$  is  $\sim 0.5\%$ . This is **about the amount needed to explain the flux anomalies observed in radio images of quasars** that are quadruply gravitationally lensed by foreground elliptical galaxies (Juerg Diemand and R. Benton Metcalf, private communications). Free streaming of WDM particles can considerably dampen the matter power spectrum in this mass range, so a WDM model with an insufficiently massive particle (sterile neutrino  $m_{\nu} < 10 \text{ keV}$ ) fails to reproduce the observed flux anomalies (Marco Miranda & Andrea Maccio 2007, MNRAS, 382, 1225). **We need more than the 6 radio quads now known!**

# The Kinematics of the Ultra-Faint Milky Way Satellites: Solving the Missing Satellite Problem

Joshua Simon & Marla Geha, ApJ 670, 313 (2007)

Hogan & Dalcanton (2000) introduced the parameter

$$Q \equiv \rho/\sigma^3$$

as an estimate of the coarse-grained phase-space density of the dark matter in galaxy halos. Liouville's theorem implies that observed values of  $Q$  set a hard lower limit on the original phase-space density of the dark matter. All of the galaxies except UMa I, CVn I, and Hercules have

$$Q > 10^{-3} M_{\odot} \text{ pc}^{-3} (\text{km s}^{-1})^{-3},$$

about an order of magnitude improvement compared to the previously-known dSphs. This places significant limits on non-CDM dark matter models.

# The Kinematics of the Ultra-Faint Milky Way Satellites: Solving the Missing Satellite Problem

Joshua Simon & Marla Geha, ApJ 670, 313 (2007)

Hogan & Dalcanton (2000) introduced the parameter

$$Q \equiv \rho/\sigma^3$$

as an estimate of the coarse-grained phase-space density of the dark matter in galaxy halos. Liouville's theorem implies that observed values of  $Q$  set a hard lower limit on the original phase-space density of the dark matter. All of the galaxies except UMa I, CVn I, and Hercules have

$$Q > 10^{-3} M_{\odot} \text{ pc}^{-3} (\text{km s}^{-1})^{-3},$$

about an order of magnitude improvement compared to the previously-known dSphs. This places significant limits on non-CDM dark matter models. **The subhalos in Via Lactea II (Diemand+2008) that could host MWy satellites have densities and phase space densities comparable to these.**

## Observational Constraints on Warm Dark Matter

Hogan & Dalcanton (2000) showed that for a thermal relic particle X

$$Q \equiv \rho/\sigma^3 = 5 \times 10^{-4} M_{\odot} \text{pc}^{-3} (\text{km s}^{-1})^{-3} (m_X/\text{keV})^4$$

Simon & Geha (2007) found  $Q > 10^{-3}$ , which implies  $m_X > 1.2 \text{ keV}$

The latest constraint from HIRES + SDSS Lyman- $\alpha$  forest data is  $m_X > 4 \text{ keV}$  (sterile neutrino  $m_\nu > 28 \text{ keV}$ ) at  $2\sigma$  (Viel+2008).

Yoshida, Sokasian, Hernquist, & Springel (2003) argued that, while the first stars can reionize the universe starting at  $z \sim 20$  in  $\Lambda\text{CDM}$ , the absence of low mass halos in  $\Lambda\text{WDM}$  delays reionization unless  $m_X > 10 \text{ keV}$ . O'Shea & Norman (2006) showed that reionization is significantly delayed in  $\Lambda\text{WDM}$  even with  $m_X = 15 \text{ keV}$ . The actual constraint on  $m_X$  has not yet been determined in detail.

If the WDM is produced by decay, the velocity distribution and phase space constraints can be different (Kaplinghat 05, **mCDM** Strigari+07).

## Observational Constraints on Sterile Neutrinos

Sterile neutrinos that mix with active neutrinos are produced in the early universe and could be the dark matter (Dodelson & Widrow 1994). However, they decay into X-rays + light neutrinos. Recent data attempting to observe these X-rays from

various sources give upper limits on  $m_s$

Virgo cluster	$< 8$ keV
Coma cluster	$< 6$ keV
X-ray background	$< 5$ keV
Milky Way	$< 3.5$ keV

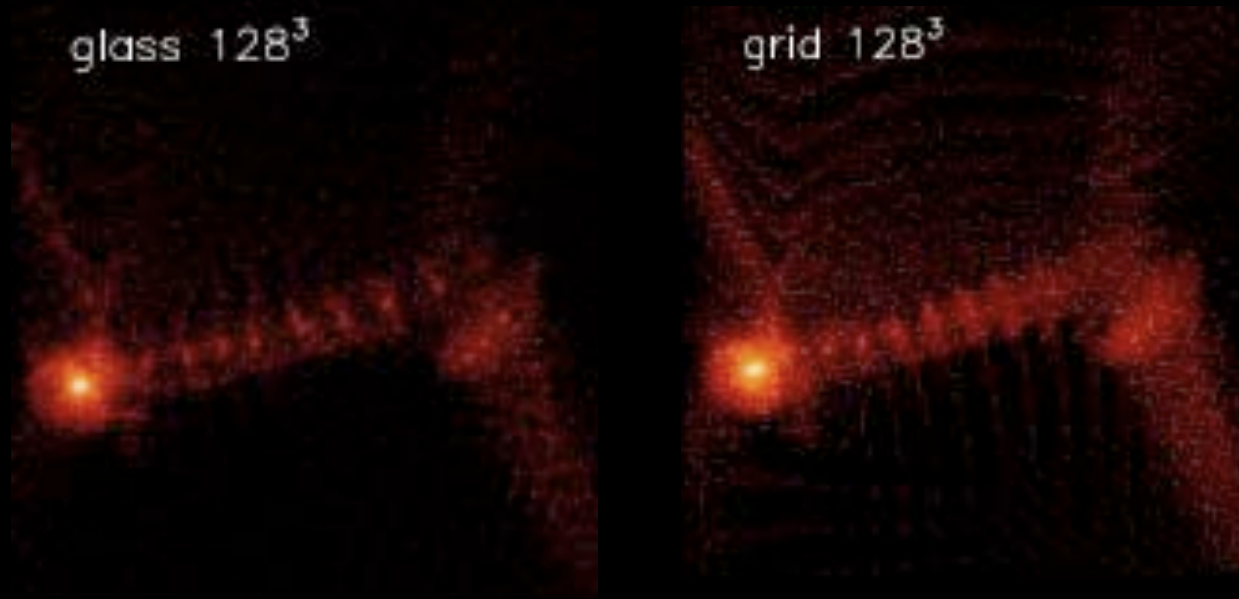
Seljak+06 and Viel+06 pointed out that these upper limits are inconsistent with the lower limits from Lyman- $\alpha$  forest data, thus **ruling out such sterile neutrinos as the dark matter**.

The latest constraint from HIRES + SDSS Lyman- $\alpha$  forest data is sterile neutrino  $m_s > 28$  keV at  $2\sigma$  (Viel+2008).



## Warm Dark Matter Substructure in Simulations

Various authors (e.g., Bode, Ostriker, & Turok 2001, Knebe, Devriendt, Gibson, & Silk 2003; Götz & Sommer-Larsen 2003) have claimed that  $\Lambda$ WDM substructure develops in simulations on scales below the free-streaming cutoff. If true, this could alleviate the conflict between the many small subhalos needed to give the observed number of Local Group satellite galaxies and needed to explain gravitational lensing flux anomalies. However, Wang & White (2007, MNRAS, 380, 93) recently showed that such **substructure** arises from discreteness in the initial particle distribution, and **is** therefore **spurious**.



# Warm Dark Matter

Lyman- $\alpha$  forest,  
satellite abundance,  
gravitational lensing,  
reionization  $\Rightarrow$

**Warm** Dark Matter

has to be rather

**Tepid**

**Hot**

**Warm** Dark Matter

has to be rather

**Tepid**

**Hot**

**Warm**

**Tepid**

**Hot**

**Warm**

**Tepid**

**Cool**

**Hot**

**Warm**

**Tepid**

**Cool**

**Cold Dark Matter**

*meta***CDM** from late decays  
can satisfy Ly $\alpha$  forest limits but  
nevertheless lead to cored dSph

## Other Challenges to $\Lambda$ CDM

- **CUSPS IN GALAXY CENTERS** Problem first recognized by Flores and me 94, and Moore 94, but HI beamsmeearing and other observational errors were underestimated (Swaters+03, Spekkens+05); the data imply inner slope  $r^{-\alpha}$   $0 \leq \alpha < 1.5$ . LSB galaxies are mainly dark matter so complications of baryonic physics are minimized, but could still be important (Rhee+04, Valenzuela+07). The only case where the Blitz group sees no radial motions is consistent with  $r^{-\alpha}$  with  $\alpha \approx 1$  (NFW) as  $\Lambda$ CDM predicts (Simon+05). The non-circular motions could be caused by nonspherical halos (Hayashi & Navarro 06). Dark matter halos are increasingly aspherical at smaller radii, at higher redshift, and at larger masses (Allgood+06, Flores+07, Bett+07), and this can account for the observed rotation curves (Hayashi+07, Bailin+07, Widrow 08).



# Structure of Dark Matter Halos

Navarro, Frenk, White

1996

1997

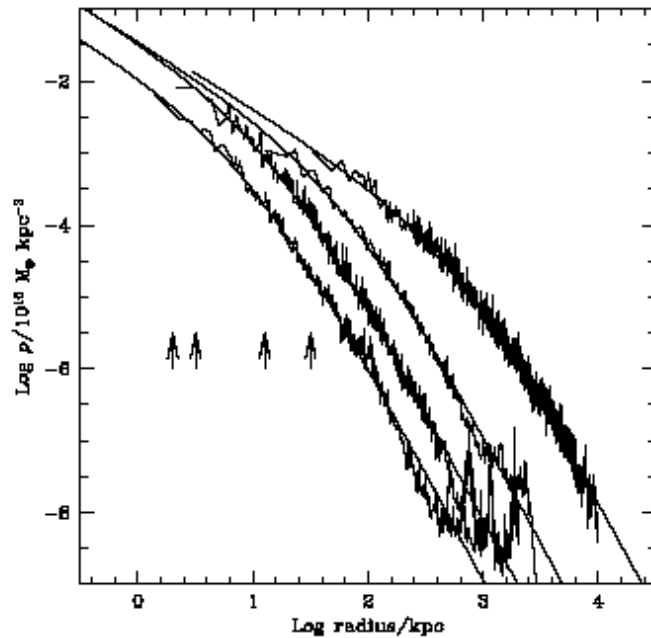
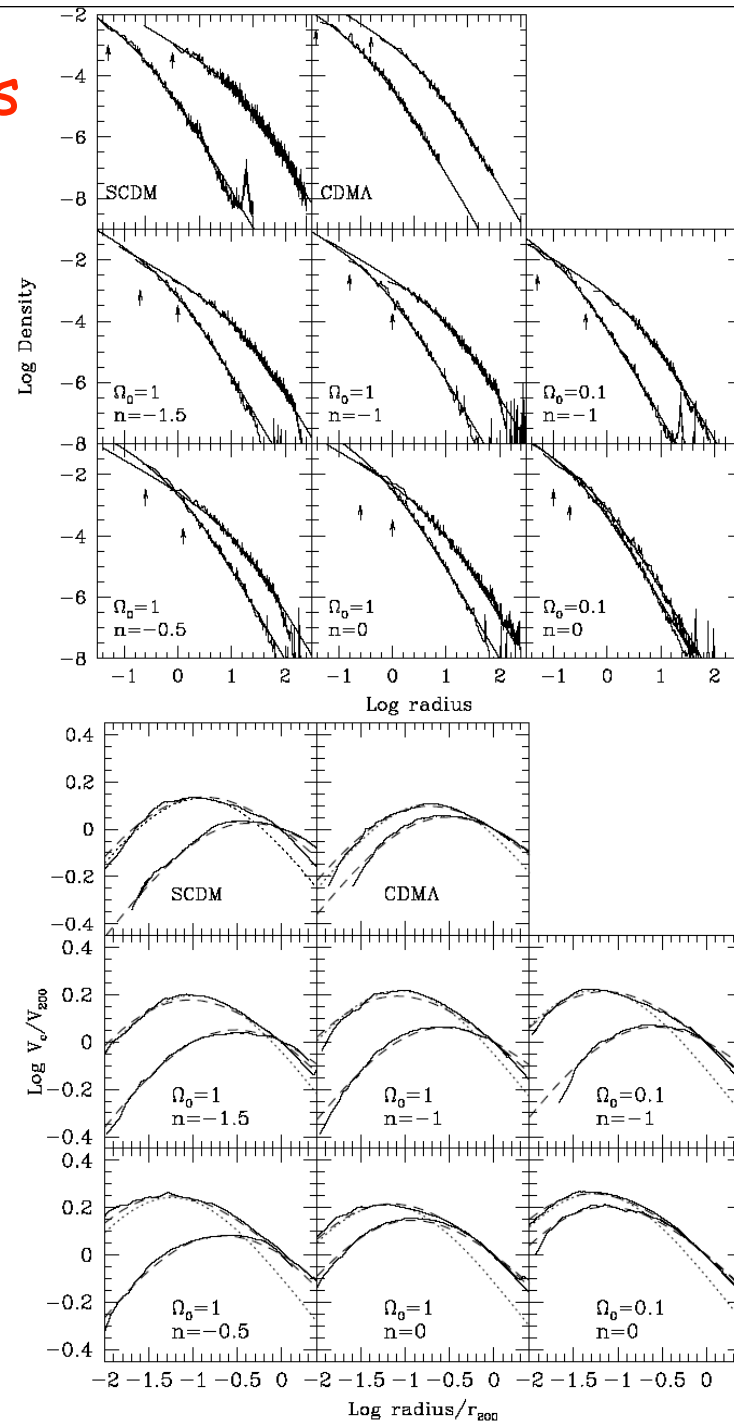


Fig. 3.— Density profiles of four halos spanning four orders of magnitude in mass. The arrows indicate the gravitational softening,  $h_g$ , of each simulation. Also shown are fits from eq.3. The fits are good over two decades in radius, approximately from  $h_g$  out to the virial radius of each system.

$$\frac{\rho(r)}{\rho_{crit}} = \frac{\delta_c}{(r/r_s)(1 + r/r_s)^2}, \quad (3)$$

NFW formula works for all models



# Dark Matter Halo Radial Profile

## COMPARISON OF NFW AND MOORE ET AL. PROFILES

Parameter	NFW	Moore et al.
Density $x = r/r_s$	$\rho = \frac{\rho_s}{x(1+x)^2}$ $\rho \propto x^{-3} \text{ for } x \gg 1$ $\rho \propto x^{-1} \text{ for } x \ll 1$ $\rho/\rho_s = 1/4 \quad \text{at } x = 1$	$\rho = \frac{\rho_s}{x^{1.5}(1+x)^{1.5}}$ $\rho \propto x^{-3} \text{ for } x \gg 1$ $\rho \propto x^{-1.5} \text{ for } x \ll 1$ $\rho/\rho_s = 1/2 \quad \text{at } x = 1$
Mass $M = 4\pi\rho_s r_s^3 f(x)$ $= M_{\text{vir}} f(x)/f(C)$ $M_{\text{vir}} = \frac{4\pi}{3}\rho_{\text{cr}}\Omega_0\delta_{\text{top-hat}}r_{\text{vir}}^3$	$f(x) = \ln(1+x) - \frac{x}{1+x}$	$f(x) = \frac{2}{3}\ln(1+x^{3/2})$
Concentration $C = r_{\text{vir}}/r_s$	$C_{\text{NFW}} = 1.72C_{\text{Moore}}$ for halos with the same $M_{\text{vir}}$ and $r_{\text{max}}$ $C_{1/5} \approx \frac{C_{\text{NFW}}}{0.86f(C_{\text{NFW}}) + 0.1363}$ error less than 3% for $C_{\text{NFW}} = 5-30$ $C_{\gamma=-2} = C_{\text{NFW}}$	$C_{\text{Moore}} = C_{\text{NFW}}/1.72$ $C_{1/5} = \frac{C_{\text{Moore}}}{[(1 + C_{\text{Moore}}^{3/2})^{1/5} - 1]^{2/3}}$ $\approx \frac{C_{\text{Moore}}}{[C_{\text{Moore}}^{3/10} - 1]^{2/3}}$ $C_{\gamma=-2} = 2^{3/2}C_{\text{Moore}}$ $\approx 2.83C_{\text{Moore}}$
Circular Velocity $v_{\text{circ}}^2 = \frac{GM_{\text{vir}}}{r_{\text{vir}}} \frac{C}{x} \frac{f(x)}{f(C)}$ $= v_{\text{max}}^2 \frac{x_{\text{max}}}{x} \frac{f(x)}{f(x_{\text{max}})}$ $v_{\text{vir}}^2 = \frac{GM_{\text{vir}}}{r_{\text{vir}}}$	$x_{\text{max}} \approx 2.15$ $v_{\text{max}}^2 \approx 0.216v_{\text{vir}}^2 \frac{C}{f(C)}$ $\rho/\rho_s \approx 1/21.3 \text{ at } x = 2.15$	$x_{\text{max}} \approx 1.25$ $v_{\text{max}}^2 \approx 0.466v_{\text{vir}}^2 \frac{C}{f(C)}$ $\rho/\rho_s \approx 1/3.35 \text{ at } x = 1.25$

Klypin, Kravtsov, Bullock & Primack 2001

# Empirical Models for Dark Matter Halos. II. Inner profile slopes, dynamical profiles, and $\rho/\sigma^3$

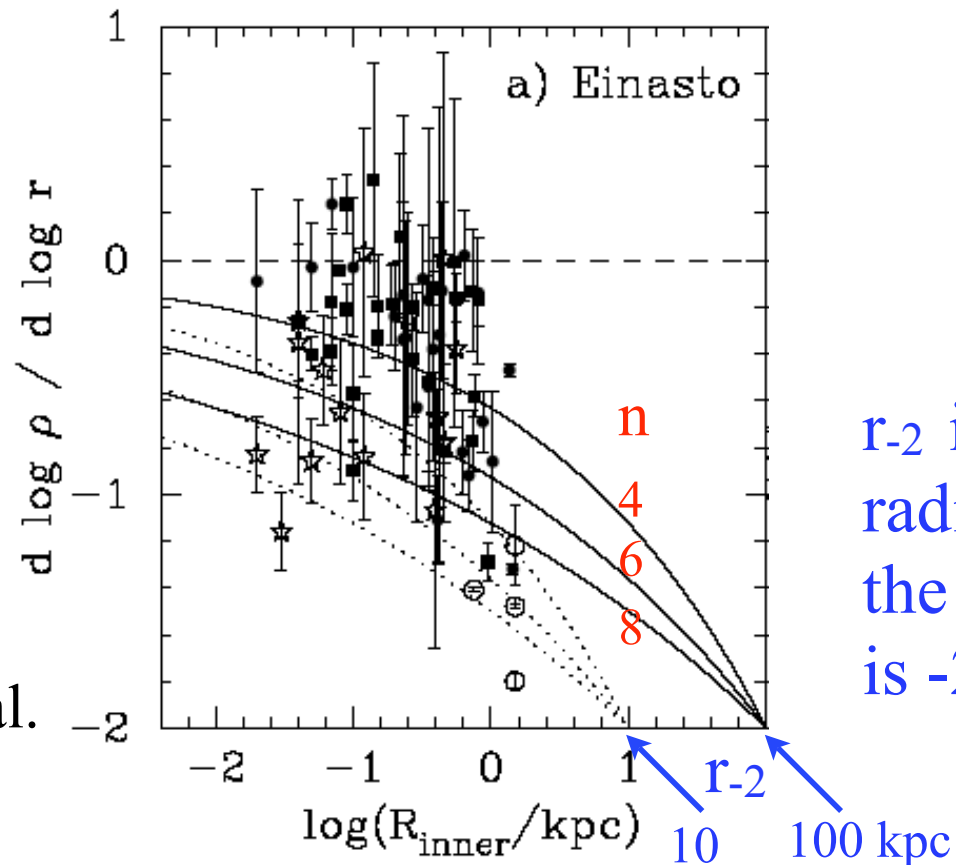
Alister Graham, David Merritt, Ben Moore, Jürg Diemand, Balša Terzić

Einasto's model is given by the equation

$$\rho(r) = \rho_e \exp \left\{ -d_n \left[ (r/r_e)^{1/n} - 1 \right] \right\}.$$

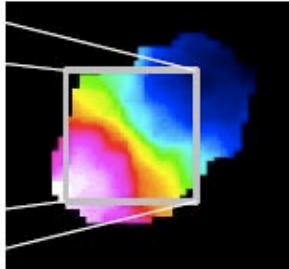
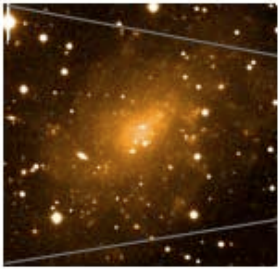
Data on log slopes from innermost resolved radius of observed galaxies, not corrected for observational effects -- adapted from de Blok (2004).

See also Navarro et al. Aquarius simulations arXiv:0810.1522



$r_{-2}$  is the radius where the log-slope is -2

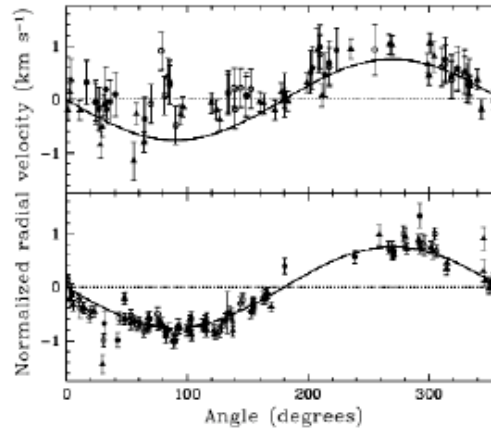
# DDO 39



Swaters, Verheijen, Bershady, Andersen 2003

# Noncircular motions

Strong noncircular motions exist even in galaxies that seem as regular as DDO 39:



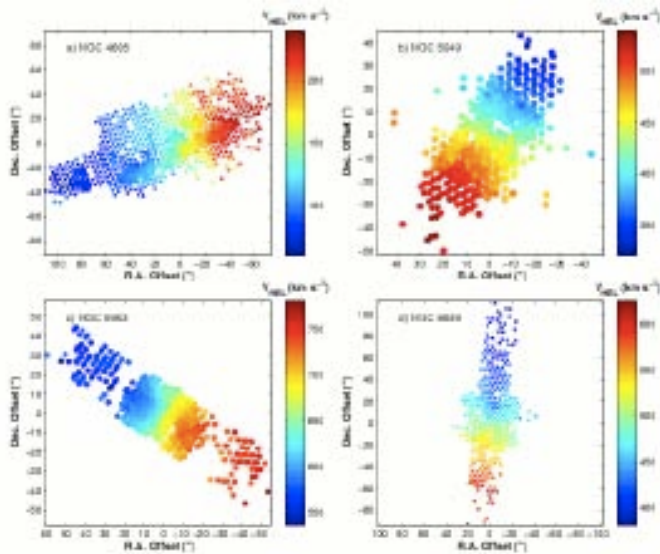
Swaters et al. 2003

Noncircular motions are common:

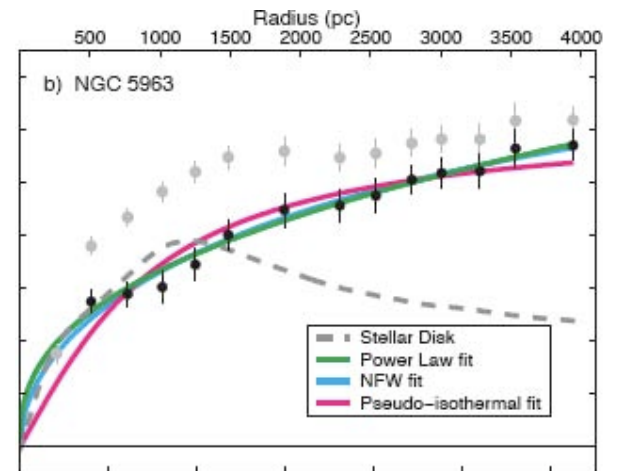
- 4 out of 5 galaxies studied by Simon et al. (2003, 2005) have detectable radial motions
- 4 out of 6 in Swaters et al. (in prep) show noncircular motions
- Majority of galaxies in GHASP survey (Garrido et al. 2003)

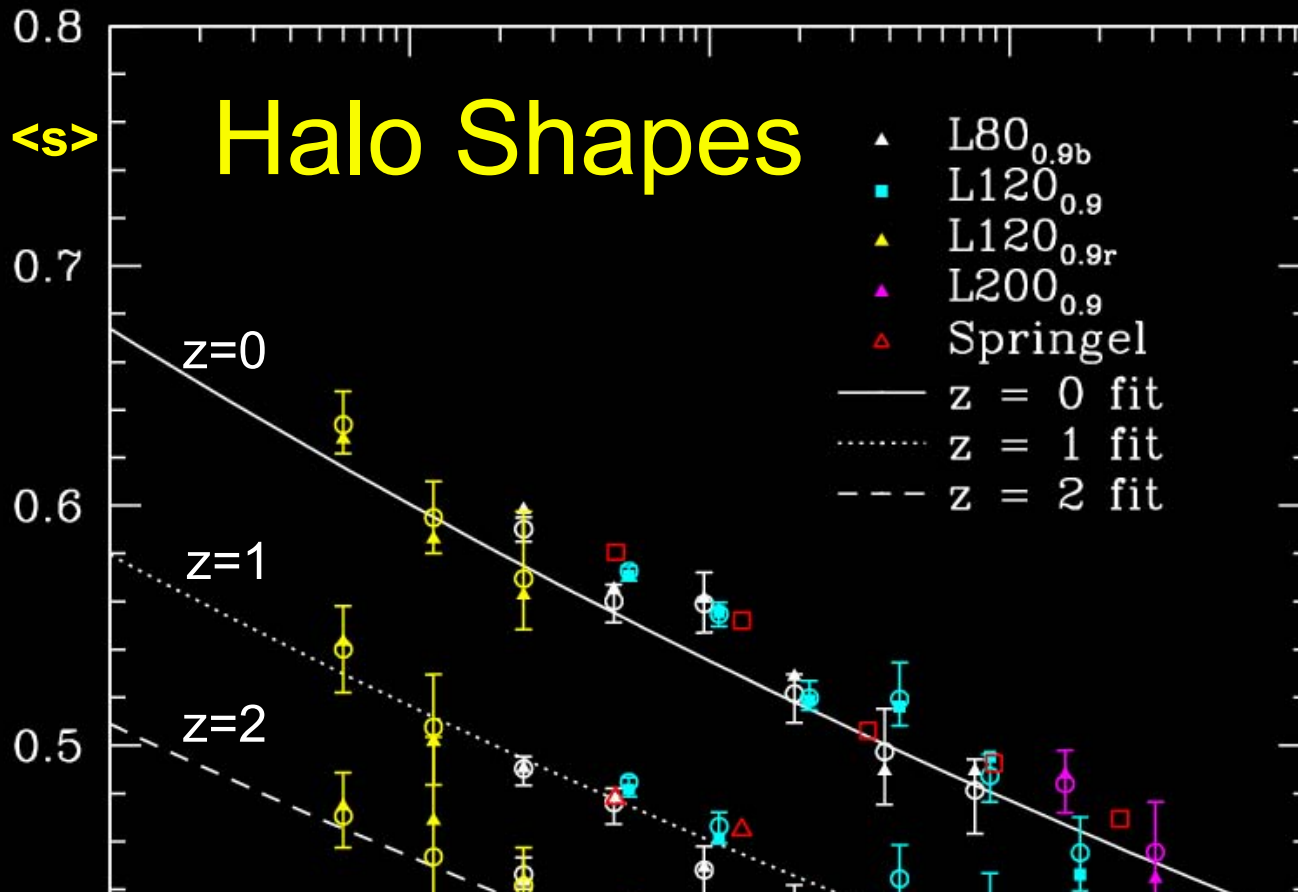
# NGC 5963

w/o radial v fits NFW



Simon+2003, 2005 obtained 2D velocity profiles of 5 low-mass spiral galaxies using CO, H $\alpha$ , and HI. They subtracted the baryons to obtain dark matter profiles.





**<math>\langle s \rangle</math> = short / long axis of dark halos vs. mass and redshift. Dark halos are more elongated the more massive they are and the earlier they form. We found that the halo <math>\langle s \rangle</math> scales as a power-law in  $M_{\text{halo}}/M_*$ . Halo shape is also related to the Wechsler halo formation scale factor  $a_c$ .**

A simple formula describes these results, as well dependence on epoch and cosmological parameter  $\sigma_8$  :

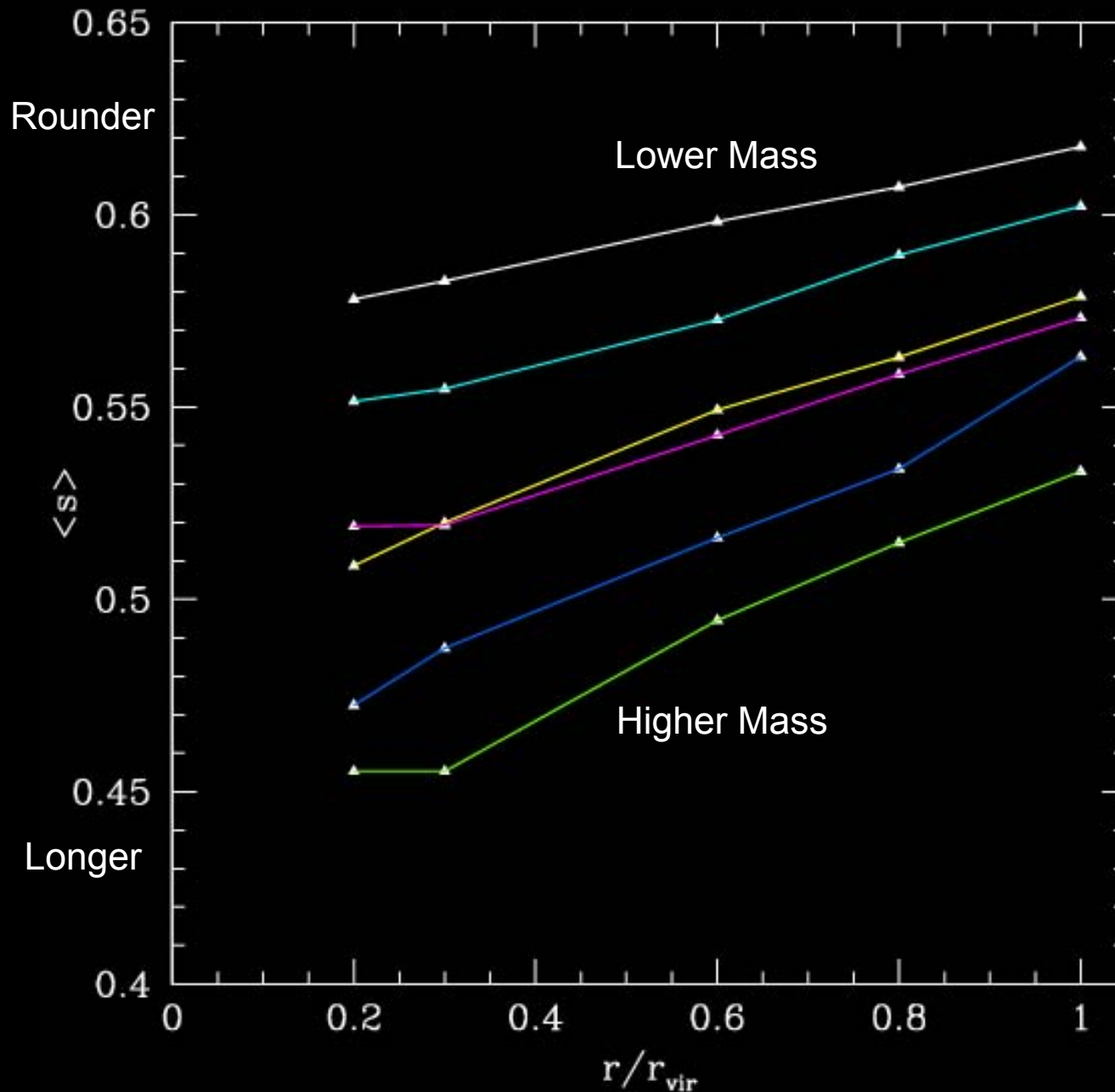
$$\langle s \rangle(M_{\text{vir}}, z = 0) = \alpha \left( \frac{M_{\text{vir}}}{M_*} \right)^\beta$$

with best fit values

$$\alpha = 0.54 \pm 0.03, \quad \beta = -0.050 \pm 0.003.$$

Allgood+2006

redshift z=0



Halos become more spherical at larger radius and smaller mass. As before,

$$s = \frac{\text{short axis}}{\text{long axis}}$$

These predictions can be tested against cluster X-ray data and galaxy weak lensing data.

Allgood+2006

## Other Challenges to $\Lambda$ CDM

- **GALAXY HALO CONCENTRATION**

It remains unclear how much adiabatic contraction (Blumenthal+86,93, Mo+98, Gnedin+04) occurs in galaxies (Dutton+08), since there are potentially offsetting effects.

Halos hosting low surface brightness (LSB) galaxies may have higher spin and lower concentration than average (Wechsler+02,06, Maccio+07), which would improve agreement between  $\Lambda$ CDM predictions and observations.

Despite all this, halos hosting galaxies may still be predicted by  $\Lambda$ CDM to be more concentrated than the data indicates (Alam+02), although lower  $P(k)$  normalization parameter  $\sigma_8$  could help (Zentner & Bullock 03, Maccio, Dutton, & van den Bosch 08). However, X-ray clusters are consistent with higher  $\sigma_8 \approx 0.9$  (Buote+07, Comerford & Natarajan 07).

# Other Challenges to $\Lambda$ CDM

- **ANGULAR MOMENTUM ISSUES**

Catastrophic **loss of angular momentum** (Navarro & Benz 91, Navarro & Steinmetz 00) due to overcooling in hydrodynamic simulations (Maller & Dekel 02). Spiral galaxies would be hard to form if ordinary matter has the same **specific angular momentum distribution** as dark matter (Bullock+01). How do the disk baryons get the right angular momentum?

**Mergers** give halos angular momentum – too much for halos that host spheroids, too little for halos that host disks (D'Onghia & Burkert 04)? Role of **AGN** and other energy inputs? Role of **cold inflows** (Birnboim & Dekel 03, Keres+05, Dekel & Birnboim 06)?

Can simulated disks agree with observed Tully-Fisher relation and Luminosity Function? Recent high-resolution simulations (Governato+07, Ceverino & Klypin 08) are encouraging (Lecture 3).





Greg Stinson, Anil Seth, Neal Katz, James Wadsley, Fabio Governato, Tom Quinn 2006

# WHAT IS THE DARK MATTER?

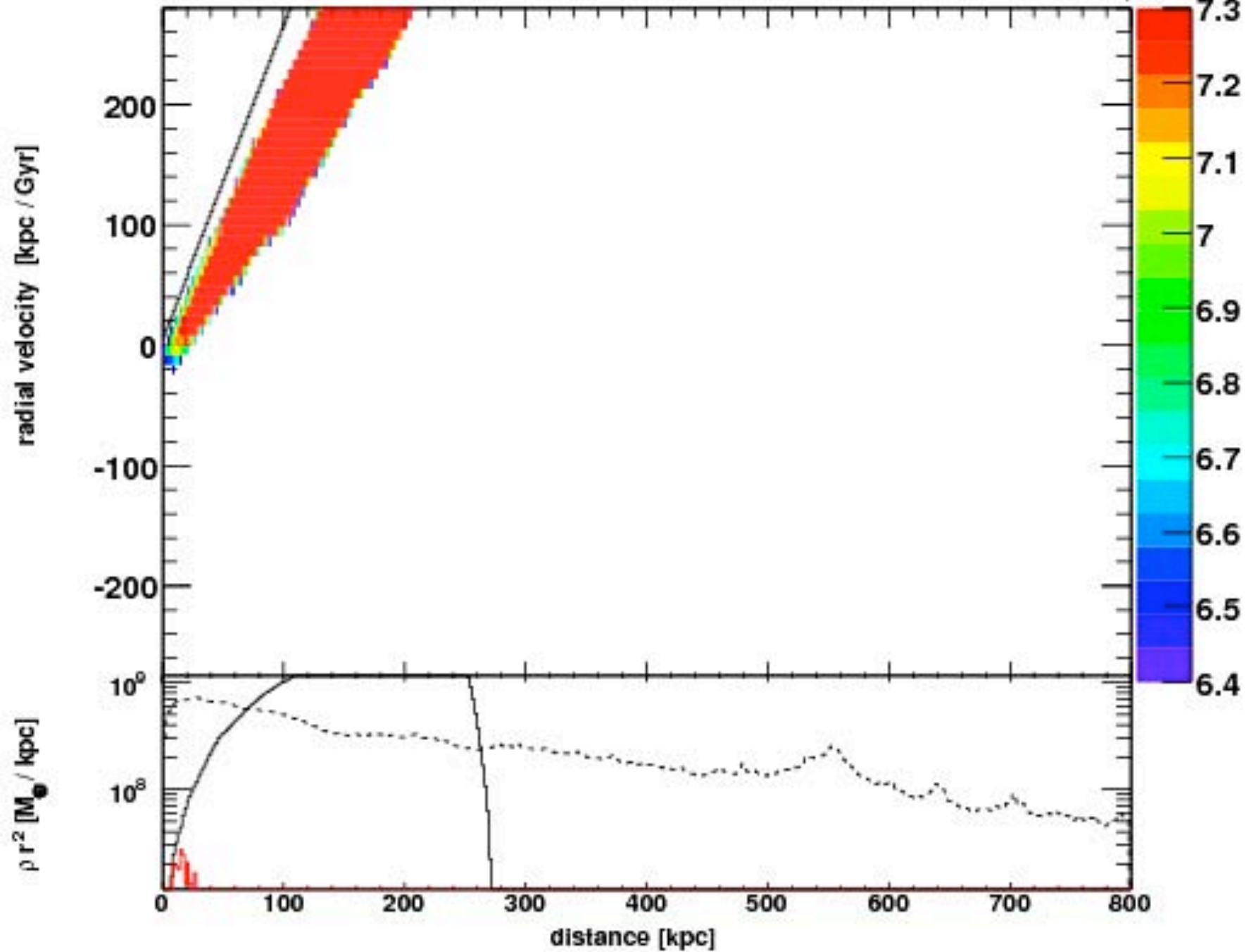
Lensing limits on MACHOs are getting stronger - skewness of high-z vs. low-z Type Ia SN disfavors  $10^{-2} < M_{\text{MACHO}}/M_{\odot} < 10^8$  (Metcalf & Silk 07).

Prospects for DIRECT and INDIRECT detection of **WIMPs** and **AXIONS** are improving... But what kind of WIMP? SUSY LSP, NLSP->LSP, KK, ...

Sikivie has claimed that caustics caused by phase wrapping as dark matter falls into the Milky Way will lead to potentially detectable effects in DM searches. This is not expected in realistic  $\Lambda$ CDM models. Caustics are seen in the Via Lactea simulation, but with very little density enhancement and only at great galactocentric distances.

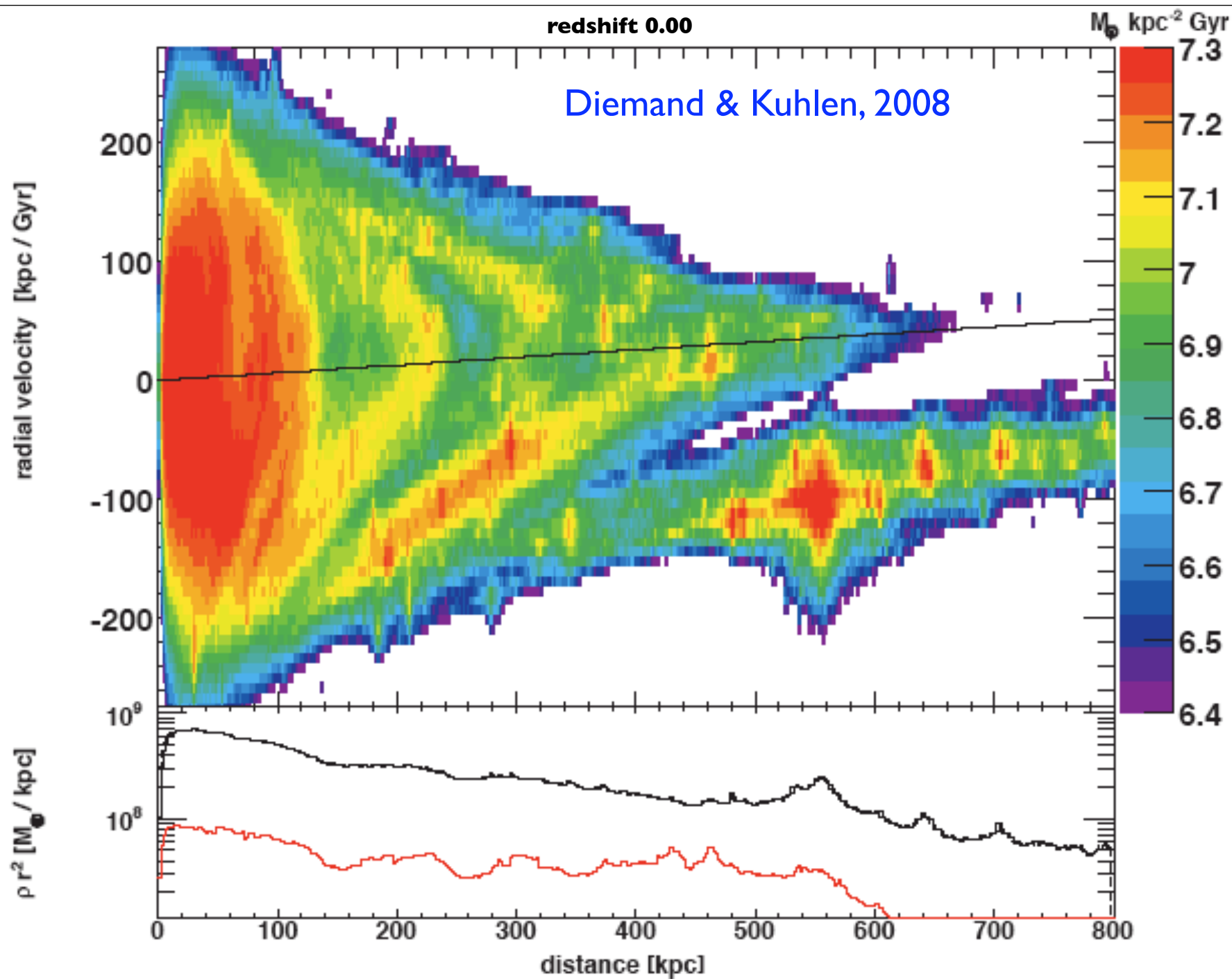
redshift 11.89

$M_{\odot} \text{ kpc}^{-2} \text{ Gyr}$



redshift 0.00

Diemand & Kuhlen, 2008



## small scale issues

### Satellites

The discovery of many faint Local Group dwarf galaxies is consistent with  $\Lambda$ CDM predictions. Reionization, lensing, satellites, and Ly $\alpha$  forest data imply that **WDM** must be **Tepid** or **Cooler**.

### Cusps

The triaxial nature of dark matter halos plus observational biases suggest that observed velocity structure of LSB and dSpiral galaxies are consistent with cuspy  $\Lambda$ CDM halos.

### Angular momentum

$\Lambda$ CDM simulations are increasingly able to form realistic spiral galaxies, as resolution improves and feedback becomes more realistic.